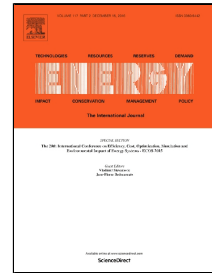


Accepted Manuscript

Effect of Split Fuel Injection and EGR on NO_x and PM Emission Reduction in a Low Temperature Combustion (LTC) Mode Diesel Engine

Ayush Jain, Akhilendra Pratap Singh, Avinash Kumar Agarwal



PII: S0360-5442(17)30050-6
DOI: 10.1016/j.energy.2017.01.050
Reference: EGY 10185
To appear in: *Energy*
Received Date: 05 October 2016
Revised Date: 17 December 2016
Accepted Date: 09 January 2017

Please cite this article as: Ayush Jain, Akhilendra Pratap Singh, Avinash Kumar Agarwal, Effect of Split Fuel Injection and EGR on NO_x and PM Emission Reduction in a Low Temperature Combustion (LTC) Mode Diesel Engine, *Energy* (2017), doi: 10.1016/j.energy.2017.01.050

This is a PDF file of an unedited manuscript that has been accepted for publication. As a service to our customers we are providing this early version of the manuscript. The manuscript will undergo copyediting, typesetting, and review of the resulting proof before it is published in its final form. Please note that during the production process errors may be discovered which could affect the content, and all legal disclaimers that apply to the journal pertain.

Effect of Split Fuel Injection and EGR on NO_x and PM Emission Reduction in a Low Temperature Combustion (LTC) Mode Diesel Engine

Ayush Jain, Akhilendra Pratap Singh, Avinash Kumar Agarwal*

Engine Research Laboratory, Department of Mechanical Engineering

Indian Institute of Technology Kanpur, Kanpur-208016, India

*Corresponding Author's email: akag@iik.ac.in

Research Highlights

- Advancing SoMI and SoPI timings improved PCCI combustion
- Retarded SoMI timings resulted in higher NO_x and PM emissions
- Increasing EGR reduced NO_x and PM mass emissions simultaneously
- Increasing EGR rate effectively controlled the HRR of PCCI combustion
- Too high EGR resulted in higher HC and CO emissions

Effect of Split Fuel Injection and EGR on NO_x and PM Emission Reduction in a Low Temperature Combustion (LTC) Mode Diesel Engine

Ayush Jain, Akhilendra Pratap Singh, Avinash Kumar Agarwal*

Engine Research Laboratory, Department of Mechanical Engineering

Indian Institute of Technology Kanpur, Kanpur-208016, India

*Corresponding Author's email: akag@iik.ac.in

Abstract

In this study, an advanced combustion concept 'premixed charge compression ignition' (PCCI) has been explored for diesel engines. PCCI combustion is a single-stage combustion process, in which a large fraction of fuel burns in premixed combustion phase resulting in relatively lower in-cylinder temperatures compared to compression ignition (CI) engine combustion. However at high loads, PCCI combustion results in severe knocking and higher oxides of nitrogen (NO_x) emissions. This limits the applicability of this combustion concept to medium loads. This limitation of PCCI combustion can be resolved by altering in-cylinder pressure-temperature history at the time of fuel injection. This can be also be resolved by deploying suitable split fuel injection strategy and exhaust gas recirculation (EGR), which control combustion events such as start of combustion (SoC) and combustion phasing, leading to lower knocking and NO_x emissions. To investigate the effects of various split injection strategy and EGR on PCCI combustion, engine experiments were conducted at different start of main injection (SoMI) timings (12, 16, 20 and 24° bTDC), start of pilot injection (SoPI) timings (30, 35 and 40° bTDC) and EGR rates (0, 15 and 30%). This study also included detailed

26 particulate characterization such as particulate number-size distribution using an
27 engine exhaust particle sizer (EEPS) and particulate bound trace metal analysis by
28 inductively coupled plasma-optical emission spectrophotometry (ICP-OES). PCCI
29 combustion was found to be superior at 35° bTDC SoPI timing and 15% EGR. At
30 retarded SoPI timing (30° bTDC), PCCI combustion resulted in slightly higher NO_x and
31 particulate emissions, however at too advanced SoPI timing (40° bTDC), PCCI
32 combustion showed relatively inferior engine performance. Application of EGR improved
33 PCCI combustion and emission characteristics, however at high EGR, PCCI combustion
34 resulted in inferior engine performance due to reduction in bulk in-cylinder
35 temperatures. Overall, this study showed that PCCI combustion stability, knocking and
36 NO_x emissions can be optimized by selecting suitable combination of SoMI and SoPI
37 timings, and EGR rate.

38

39 **Keywords:** Partially premixed charge compression ignition; Heat release rate; Exhaust
40 gas recirculation; Split injection; Knocking.

41

42 **1. Introduction**

43 Rapid technological and economic advances in last few decades have culminated in
44 rapid depletion of petroleum resources. In transport sector, compression ignition
45 (CI) engines are being widely used currently, especially in light-duty and heavy-
46 duty vehicles because of their higher thermal efficiency, greater reliability and
47 superior fuel economy compared to gasoline engines. However CI engines suffer
48 from major drawbacks of high oxides of nitrogen (NO_x) and particulate matter (PM)
49 emissions, which limit their applications due to prevailing stringent emission norms
50 globally. Trade-off between PM and NO_x is the main challenge faced by CI engines.
51 The PM-NO_x dilemma in CI engines was first addressed by Akihama et al. [1]. They

52 suggested that application of exhaust gas recirculation (EGR) might be one of the
53 possible solutions for this problem and experimentally studied the effects of ultra-
54 high EGR on diesel combustion for simultaneous reduction in both NO_x and PM.
55 Too high EGR deteriorates the combustion characteristics and subsequently the
56 engine performance; therefore different researchers coupled EGR with advanced
57 combustion techniques such as homogeneous charge compression ignition (HCCI).
58 HCCI emerged in the late 1970's, when Onishi et al. [2] experimentally
59 demonstrated this novel combustion concept in a two-stroke engine. This concept
60 was further explored by Thring [3], and HCCI combustion was implemented in a
61 four-stroke engine. After these pioneering research efforts, several other researchers
62 including Christensen et al. [4], Stanglmaier et al. [5] and Maurya et al. [6]
63 successfully demonstrated HCCI combustion concept in spark ignition (SI) engines.
64 In 1990's, efforts were made to examine and deploy this concept in diesel engines.
65 Singh et al. [7] reported combustion characteristics of diesel HCCI engine. Even
66 though HCCI concept proved to be effective in reducing NO_x emissions from diesel
67 engines, there were significant unresolved issues related to start of combustion
68 (SoC), combustion phasing and, high hydrocarbons (HC) and carbon monoxide (CO)
69 emissions [8]. These challenges motivated researchers to develop a new low
70 temperature combustion (LTC) strategy, known as premixed charge compression
71 ignition (PCCI) combustion. In PCCI combustion, fuel is injected at an intermediate
72 timing between that of HCCI and conventional CI combustion. Advanced start of
73 injection (SoI) timing results in a partially premixed fuel-air mixture due to
74 relatively lesser time available compared to HCCI combustion. Therefore, PCCI
75 combustion can be considered as a 'premixed combustion phase dominated CI
76 combustion'. Due to low volatility of mineral diesel, diesel fuelled PCCI combustion
77 investigations mainly focused on high pressure direct fuel injection strategies

78 employing EGR [1, 9-12]. Higher fuel injection pressures and enhanced swirl ratios
79 promoted fuel-air mixing however sufficient premixing time between end of injection
80 (EoI) and SoC was necessary for achieving efficient PCCI combustion [13].

81 Initially, single stage direct injection of fuel was employed to achieve PCCI
82 combustion wherein early direct injection during the compression stroke promoted
83 fuel-air mixing due to presence of higher in-cylinder temperature and longer charge
84 premixing time. However too advanced SoI timings resulted in fuel spray
85 impingement on the walls resulting in cylinder wall wetting, leading to incomplete
86 combustion and subsequently reduced thermal efficiency as well as higher HC
87 emissions [14-15]. In PCCI combustion, fuel-air mixture homogeneity was also
88 significantly affected by in-cylinder conditions (pressure-temperature history). For
89 controlling the in-cylinder conditions at the time of main injection, researchers
90 employed split fuel injection. Hashizume et al. [14] proposed a concept of 'multiple
91 stage diesel combustion' (MULDIC), in which two-stage fuel injection was
92 implemented to achieve the LTC. Using MULDIC, they achieved significant
93 reduction in NO_x and soot emissions simultaneously, however fuel economy was
94 inferior compared to conventional CI combustion. Neely et al. [15] investigated
95 effect of pilot injections (up to 3) to achieve PCCI combustion in light and heavy-
96 duty vehicles. In case of single pilot injection, they observed considerable reduction
97 in NO_x emissions however higher CO emission. This CO penalty was reduced by
98 implementing multiple pilot injections. Effect of split injection strategy on NO_x
99 formation was explored by Horibe et al. [16] and Torregrosa et al. [17]. They
100 reported that higher thermal efficiency and lower NO_x emissions at moderate
101 engine loads could be achieved by single pilot injection however excessive rate of
102 pressure rise (RoPR) limited the operating window of the PCCI combustion. In order
103 to control the RoPR of PCCI combustion, researchers suggested using EGR. Higher

104 level of EGR was used to achieve longer ignition delay (to improve fuel-air mixing)
105 and lower in-cylinder temperature (to reduce NO_x emissions) simultaneously [18].
106 However very high level of EGR increased HC and CO emissions and reduced the
107 thermal efficiency. Kook et al. [19] and Kanda et al. [20] conducted experiments
108 using different dilution rates (EGR) to attain PCCI combustion. High heat capacity
109 of diluting gas lowered the adiabatic flame temperature, which prevented NO_x
110 formation. These researchers reported that NO_x and soot luminosity had direct
111 correlation with the adiabatic flame temperature and it decreased with increasing
112 EGR rate. Manente et al. [21] examined the physical and chemical concepts of EGR
113 on engine-out emissions in a PCCI engine. They reported that increasing EGR did
114 not affect engine efficiency however it decreased CO and HC emissions significantly.
115 Detailed study of injection parameters and fuel spray impingement on emission
116 characteristics of mineral diesel fuelled PCCI engines was performed by Kiplimo et
117 al. [22]. They observed that an increase in fuel injection pressure (FIP) led to lower
118 HC, PM and NO_x emissions with no change in CO emission. EGR stratification was
119 a novel approach demonstrated by Andre et al. [23] and it was used to control rapid
120 heat release and combustion noise in a LTC engine. Jacobs et al. [24] and Hardy et
121 al. [25] investigated lean PCCI combustion for controlling NO_x and PM emissions
122 simultaneously. Lean PCCI combustion was achieved by employing high EGR rates,
123 higher FIP and SoI timings close to TDC. This strategy reduced NO_x and PM
124 emissions because in-cylinder conditions were not favorable for formation of soot
125 particles in the combustion chamber in case of LTC. None of these studies discussed
126 effects of fuel injection parameters and EGR on particulate composition.

127 Many researchers showed that particulate emitted by PCCI combustion were
128 significantly lower therefore detailed particulates characterization remained
129 a rather ignored area by the researchers. However hypothesis of generating

130 negligible particulate from LTC was contradicted by Price et al. [26]. This was
131 supported by experimental studies of Kittelson and Franklin [27]. Agarwal et al.
132 [28] also undertook comprehensive experimental investigations to characterize
133 exhaust particulate from a mineral diesel fuelled LTC engine. It was amply
134 demonstrated without any doubt that the relative air-fuel ratio (λ) and EGR were
135 the major governing factors that affect particulate emissions from the LTC engine.
136 Further, the effect of intake air pressure and oxygen content of the inlet air on
137 particulate size-number distribution was investigated by Desantes et al. [29]. They
138 reported that a slight increase in inlet air oxygen content caused significant
139 reduction in CO, HC, and PM mass and particulate number emissions. Khalek et al.
140 [30] observed the influence of inlet air dilution (EGR) on particulate emissions from
141 a mineral diesel fuelled HCCI engine. They reported that dilution air temperature,
142 dilution ratio and relative humidity were quite important for the formation of
143 nucleation mode particulate ($D_p < 50$ nm). However accumulation mode particulate
144 formation was less dependent on dilution conditions. Idicheria et al. [31] examined
145 soot formation in PCCI combustion at very high EGR rates and reported that an
146 increase in ambient temperature resulted in higher soot formation in presence of
147 high EGR rate compared to no EGR case. Researchers also reported that particulate
148 composition was different in case of LTC compared to CI combustion [28], due to
149 different combustion characteristics of LTC. Among composition of particulate, trace
150 metals, polycyclic aromatic hydrocarbons (PAHs) and benzene soluble organic
151 fraction (BSOF) content are important. Springer [32] carried out experiments to
152 evaluate particulate bound trace metals from light-duty and heavy-duty diesel
153 engines. He reported that presence of trace metals like calcium, sodium,
154 phosphorus, zinc, silicon, etc., were strongly affected by in-cylinder conditions
155 during combustion. Agarwal et al. [28] also investigated particulate bound trace

156 metals from mineral diesel fuelled LTC engine. They reported that most of trace
157 metals mainly originated from incomplete combustion of fuel (trace metals in fuel),
158 wear of engine components and pyrolysis of lubricating oil (from organo-metallic
159 additives). However detailed analysis of particulate such as trace metals emitted
160 from PCCI engines has not been thoroughly investigated.

161 All these studies indicated that fuel injection timing, strategy and charge dilution affect
162 combustion, performance, emissions and particulate characteristics of a LTC engine.
163 These studies were carried out by considering variations in each parameter separately.
164 However combined effect of these parameters was not explored. This study evaluates the
165 effects of split injection and EGR on combustion, performance, emissions and particulate
166 characteristics simultaneously. The experiments were carried out in a single cylinder
167 research engine operated in PCCI combustion mode. Detailed particulate
168 characterization including particulate number-size distribution and particulate bound
169 trace metal analysis was done. These are the innovative aspects of this experimental
170 investigation, which were not been explored by previous studies given in open literature.
171 To support the particulate characterization results, detailed analysis of combustion,
172 performance and emission characteristics of PCCI combustion has been also carried out
173 as well. Effects of SoPI and SoMI timings and EGR on NO_x-PM trade-off is another
174 important aspect of this study.

175

176 **2. Experimental Setup**

177 In this experimental study, a single cylinder direct injection compression ignition (DICI)
178 research engine (AVL List GmbH; 5402) was used to perform PCCI experiments. This
179 test engine was a single cylinder version of a four-cylinder automotive high-speed direct
180 injection (HSDI) diesel engine and was equipped with a modern common rail direct
181 injection (CRDI) system. The mechanical dynamics of the engine was made similar to a

182 multi-cylinder engine using first order force balancers. A transient (AC) dynamometer
183 (Wittur Electric Drives GmbH, 2SB-3) was used to control the engine speed and torque.
184 The engine was equipped with a fuel measurement unit, a fuel conditioning unit, a
185 chiller unit, a coolant conditioning system and a lubricating oil conditioning system for
186 carrying out all investigations under controlled experimental conditions. During entire
187 experiment, the lubricating oil and fuel temperatures were maintained at 90° and 25°C
188 respectively. For combustion analysis, a water-cooled piezoelectric pressure transducer
189 (AVL, QC34C) was installed in the engine cylinder head. Rotation of the crankshaft was
190 monitored using an optical encoder (AVL, 365C). Cylinder pressure-crank angle data
191 was acquired and analyzed by a high speed combustion data acquisition system (AVL,
192 IndiMicro). Schematic of the experimental setup is shown in Figure 1 and the technical
193 specifications of the engine are given in Table 1.

194 Figure 1: Schematic of the experimental setup

195 Table 1: Technical specifications of the test engine

196 Engine management system (EMS) of this engine had flexibility to control and measure
197 fuel injection parameters in manual mode of operation. Flexible fuel injection system of
198 EMS was capable of employing 4 injections in a cycle, including 2 pilots, 1 main and 1
199 post injection. An open loop fuel injection control strategy was loaded in the ETAS
200 system to control fuel injection parameters independently. This control system consisted
201 of an electronic control unit (ECU), a communication interface (ETAS, ETK 7.1) and an
202 INCA software program. The injection parameters for each injection event could be
203 modified and logged independently through the INCA software, which was used to
204 communicate with the ETAS system.

205 To control PCCI combustion, a fraction of exhaust gas (coming directly from the engine)
206 was recirculated back into the intake manifold. For controlling the EGR, a control valve
207 was installed in the EGR loop. EGR rate was measured by reduction in mass flow rate of

208 fresh intake air since reduction in mass flow rate of fresh air was directly proportional
209 to the EGR. Quantity of fuel supplied to the engine was measured using a Coriolis force
210 based fuel metering unit (AVL, 733s). This system performs continuous measurement of
211 weight of a measuring vessel, through which fuel is supplied to the engine. To measure
212 gaseous emission concentrations, a raw exhaust emission analyzer (Horiba, ESXA-1500)
213 was used. This equipment comprised of a CO/ CO₂ analyzer (NDIR detector: MCA-
214 220UA), O₂ analyzer (Paramagnetic pressure detector: MCA-220UA), HC analyzer (Hot
215 flame ionization detector: FIA-225UA) and NO_x analyzer (Chemiluminescence detector:
216 CLA-220UA). Opacity of exhaust was measured by a smoke opacimeter (AVL; 437).
217 Particulate emission characterization was done using an engine exhaust particle sizer™
218 (EEPS) (TSI Inc.; 3090), which was capable of measuring particle sizes ranging from 5.6
219 - 560 nm and particle concentrations up to 10⁸ particles/ cm³ of exhaust gas. For
220 particulate composition analysis, a partial flow dilution tunnel was used to collect the
221 particulate emitted by the engine on a preconditioned filter paper. Particulate loaded
222 filters were analyzed for trace metals using inductively coupled plasma optical emission
223 spectrophotometer (ICP-OES) (Thermo Fischer Scientific, iCAP DUO 6300 ICP
224 Spectrophotometer).

225

226 **3. Results and Discussion**

227 Objectives of this study were to select a suitable split injection strategy and optimum
228 EGR rate, which could deliver lower NO_x and PM emission and control the engine
229 knocking. To attain this objectives, PCCI experiments were performed at varying SoPI
230 timings (30, 35 and 40° bTDC), SoMI timings (12, 16, 20 and 24° bTDC) and EGR rates
231 (0, 15 and 30%). During entire set of experiments, FIP and engine speed were
232 maintained constant at 700 bar and 1500 rpm respectively and mineral diesel was used
233 as test fuel. Results obtained from the experiments were divided into five categories

234 namely: combustion, performance, emissions, particulate characteristics and particulate
235 bound trace metals and the main outcome of this study was summarized as statistical
236 plots between PM and NO_x emissions.

237

238 **3.1 Combustion Characteristics**

239 Parameters such as in-cylinder pressure history, heat release rate (HRR), SoC, etc., are
240 very effective tools for analyzing the engine combustion characteristics. In this study,
241 pressure-crank angle data was acquired by a high speed data acquisition system. To
242 eliminate cycle-to-cycle combustion variability, average data set of 250 consecutive
243 engine cycles was used for detailed combustion analysis.

244 Figure 2: Variations in cylinder pressure and HRR w.r.t. crank angle at different SoPI
245 and SoMI timings

246 Figure 2 shows the variation in cylinder pressure and HRR at different SoPI and SoMI
247 timings. At each SoPI timing, SoMI timings sweep was taken from 12 to 24° bTDC.
248 During experiment, 15% EGR rate was maintained. Results obtained showed that
249 advancing SoMI timing improved PCCI combustion due to longer time availability for
250 fuel-air mixing. At advanced SoMI timings (20 and 24° bTDC), peak in-cylinder pressure
251 (P_{max}) and peak HRR increased and shifted towards bTDC. This indicated higher
252 premixed combustion tendency at advanced SoMI timings. At advanced SoMI timings,
253 main combustion duration also reduced (reduced HRR curve width) due to faster fuel-air
254 chemical kinetics. These trends are similar to those reported by Zhao et al. [33].
255 Advancing SoPI timings affected PCCI combustion in two ways: (i) advanced SoPI
256 timings provided longer time for in-cylinder conditioning, which resulted in
257 homogeneous fuel-air mixture and improved PCCI combustion, and (ii) too advanced
258 SoPI timings led to inferior fuel-air mixing due to lower in-cylinder temperature and
259 pressure. In presence of lower in-cylinder temperature, fuel vaporization decreased.

260 However lower in-cylinder pressure deteriorated fuel spray characteristics (relatively
261 bigger fuel droplets leading to longer spray tip penetration and smaller spray area),
262 which ultimately affected fuel-air mixing characteristics [34]. Dominance of these two
263 factors can be clearly seen from the trends for in-cylinder pressure. At 30° bTDC SoPI
264 timings, less time availability for in-cylinder conditioning resulted in slightly lower
265 P_{max} , higher HRR and higher RoPR (steeper in-cylinder pressure curves). At 40° BTDC
266 SoPI timing, slightly inferior in-cylinder conditions dominated over the time availability
267 factor, resulting in lower P_{max} , HRR and RoPR (flatter in-cylinder pressure curves).
268 Ganesh et al. [35] performed similar experiments and observed similar combustion
269 characteristics. Amongst all SoPI timings, 35° bTDC showed trade-off between the above
270 two factors, which resulted in slightly higher (~2-3 bar) P_{max} compared to 30 and 40°
271 bTDC. With advancing SoPI timings, slightly advanced SoC was another important
272 observation. This indicated that SoPI timing controlled the chemical kinetics of the fuel-
273 air therefore it can be used to control PCCI combustion.

274 Figure 3 shows the variation in cylinder pressure and HRR at different EGR rates and
275 SoMI timings. At each EGR rate, SoMI timings were varied from 12 to 24° bTDC.
276 During these experiments, SoPI timing was maintained constant at 35° bTDC.
277 Variations in combustion characteristics at different SoMI timings were similar to those
278 observed in case of varying SoPI timings, however effects of varying SoMI timings were
279 greater at higher EGR rates. This was mainly due to relatively lesser fuel quantity and
280 lower in-cylinder temperatures at higher EGR rates.

281 Figure 3: Variation in cylinder pressure and HRR w.r.t. crank angle for different SoMI
282 timings and EGR rates

283 Results obtained showed that P_{max} and maximum HRR decreased with increasing EGR
284 rate. Exhaust gas consists of primarily inert species therefore increasing EGR rate
285 reduced the oxygen content of intake air, resulting in relatively lower chemical kinetics

286 of fuel-air mixtures. Presence of gaseous species with high heat capacity such as CO₂,
 287 water vapor, etc., in exhaust gas led to absorption of combustion generated heat thus
 288 lowering the P_{max} and HRR. This is the main reason for lower NO_x formation at higher
 289 EGR rates. Retarded SoC with increasing EGR rate was another important observation
 290 of this study. With increasing EGR rate, presence of inert species in the exhaust gas led
 291 to longer ignition delay and subsequently retarded the SoC timings. Effect of EGR rate
 292 on combustion stability and knocking characteristics can also be observed from the
 293 trends of cylinder pressure and HRR. At 0% EGR rate, HRR was too high, which led to
 294 noisy combustion. With increasing EGR rate, combustion knock reduced. However at
 295 very high EGR rate (~30%), combustion became too slow, which deteriorated the PCCI
 296 engine performance and resulted in higher HC emissions. Amongst all the three EGR
 297 rates, 15% EGR rate was found to be the most suitable for PCCI combustion because it
 298 exhibited a trade-off between combustion and performance characteristics.

299 Figure 4: SoC, combustion phasing and combustion duration w.r.t. SoMI timings at
 300 different (a) SoPI timings and (b) EGR rates

301 Figure 4 (a) shows variation in SoC, combustion phasing and combustion duration at
 302 different SoMI and SoPI timings. These parameters were calculated from mass fraction
 303 burned (MFB) analysis. MFB was calculated by Rosswailer and Withrow method [36] as
 304 given below:

$$(\Delta p_c) = p_i - p_{i-1} \left(\frac{V_{i-1}}{V_i} \right)^\gamma$$

305 Here Δp_c is the increase in cylinder pressure due to combustion and γ is the polytropic
 306 exponent. Using this relation, MFB can be computed as:

$$\frac{m_{b(i)}}{m_{b(total)}} = \frac{\sum_{j=0}^i \Delta(p_c)_j}{\sum_{j=0}^N \Delta(p_c)_j}$$

308

309 Here it is assumed that sample 0 is between inlet valve closing and SoC and sample N is
310 after the completion of combustion.

311 In the current study, crank angle position corresponding to 10% MFB (CA_{10}) was
312 considered as SoC. In PCCI combustion, combustion started well before TDC ($\sim 2-10^\circ$
313 bTDC) due to advanced SoMI timings and faster chemical kinetics of fuel-air mixture.
314 Advancing SoMI timing from 12 to 24° bTDC also resulted in advanced SoC. This trend
315 was also visible from cylinder pressure and HRR curves. Advancing SoPI timings
316 resulted in slightly advanced SoC. This was attributed to improved fuel-air mixing due
317 to longer time availability. The difference between SoC timings at different SoPI timings
318 increased at advanced SoMI timings. This showed that advanced SoPI timing was more
319 effective at advanced SoMI timings ($\sim 20-24^\circ$ bTDC) compared to retarded SoMI timings
320 ($\sim 12-16^\circ$ bTDC). 30 and 35° bTDC SoPI timings resulted in almost similar SoC, however
321 40° bTDC SoPI timing resulted in slightly advanced SoC. This showed that chemical
322 kinetics of fuel-air mixture was not significantly affected by fuel-air premixing, but was
323 significantly affected by in-cylinder conditions. This could be clearly observed from the
324 combustion phasing results. Crank angle position corresponding to 50% MFB (CA_{50}) was
325 taken as combustion phasing. Combustion phasing affected PCCI combustion efficiency,
326 which decreased for too advanced as well as too retarded combustion phasing. Advanced
327 combustion phasing led to higher HRR which resulted in excessive knocking. However
328 late combustion phasing led to inferior combustion, which resulted in higher HC and CO
329 emissions. Combustion phasing also followed similar trend at different SoMI and SoPI
330 timings as that of SoC. However differences between combustion phasing at different
331 SoPI timings were relatively lower compared to that of SoC. In PCCI combustion,
332 combustion phasing was significantly advanced compared to CI combustion [37]. This
333 was attributed to dominance of premixed combustion phase, which resulted in relatively
334 faster combustion compared to CI combustion. Combustion duration is defined as the

335 crank angle difference between 10 and 90% MFB ($CA_{90} - CA_{10}$). In PCCI combustion,
336 variation in combustion duration shows the rapidness of combustion. Results obtained
337 showed that combustion duration of PCCI combustion (~10-20 CAD) was significantly
338 shorter compared to CI combustion (~30-40 CAD). This was mainly due to absence of
339 diffusion combustion phase (slower combustion) in PCCI mode. With advanced SoMI
340 timings, combustion duration slightly decreased. This trend also validated previous
341 observation of relatively faster chemical kinetics of fuel-air mixture at advanced SoMI
342 timings. Combustion duration slightly decreased at advanced SoPI timings though the
343 difference was not significant. At all SoPI timings, combustion duration varied from
344 ~12-17 CAD.

345 Figure 4 (b) shows the variation in SoC, combustion phasing and combustion duration at
346 different SoMI timings and EGR rates. In the experiment, SoPI timing was maintained
347 constant at 35° bTDC. At 0% EGR rate, SoC was significantly advanced compared to 15
348 and 30% EGR rates. This was mainly due to presence of relatively higher fuel quantity,
349 which enhanced chemical kinetics of fuel-air mixtures, resulting in advanced SoC.
350 Combustion phasing also varied similar to SoC. Increasing EGR rate led to relatively
351 advanced combustion phasing. These observations showed that EGR affected both, the
352 fuel-air mixing (hence SoC), as well as the chemical kinetics of fuel-air mixture (i.e.
353 combustion phasing). At 30% EGR rate, combustion phasing retarded due to slower
354 chemical kinetics of fuel-air mixture. At higher EGR rates, presence of inert gaseous
355 species reduced the reaction kinetics of fuel-air mixture and reduced the in-cylinder
356 temperature further, thus retarding the combustion phasing. With increasing EGR rate,
357 combustion duration slightly increased, however the difference in combustion duration
358 at different EGR rates was negligible. Combustion duration in PCCI combustion was
359 controlled by two factors: (i) with increasing EGR rate, slower fuel-air chemical kinetics
360 increased the combustion duration, and (ii) presence of lower fuel quantity decreased the

361 combustion duration. Due to these two counter effects of EGR, combustion duration
362 remained almost constant for different EGR rates. The results obtained by Hardy et al.
363 [25] were also similar to these findings. Figure 5 shows the variation in knocking
364 integral (KI), knock peak (KP) and combustion noise at different SoPI timings and EGR
365 rates.

366 KI is the integral of superimposed, rectified knock oscillations and KP reflects absolute
367 maxima of the rectified knock oscillations superimposed on the in-cylinder pressure
368 traces. To calculate these parameters, in-cylinder pressure signal was filtered through a
369 high pass filter and then rectified. Parameters such as KI or KP of the superimposed
370 oscillations were determined from these signals. Cylinder noise levels were calculated
371 from the cylinder pressure signals.

372 Figure 5 (a) shows the variations in KI, KP and combustion noise w.r.t. SoMI and SoPI
373 timings. In PCCI combustion, KI has been shown to be very low compared to CI or HCCI
374 combustion [38] and this was attributed to presence of pilot fuel injection, which
375 improves fuel-air mixing due to higher in-cylinder temperatures. In this study,
376 application of EGR further improved the PCCI knocking characteristics due to relatively
377 slower chemical kinetics of fuel-air mixtures. With advancing SoMI timing, KI slightly
378 decreased with almost negligible variations. Advancing SoPI timing didn't affect KI
379 significantly.

380 Figure 5: Variation in knock integral, knock peak and combustion noise w.r.t. SoMI
381 timings at different (a) SoPI timings and (b) EGR rates

382 Similar to KI, KP was also low for PCCI combustion. Advancing SoMI or SOPI timings
383 also did not affect KP significantly, though it decreased slightly. This was attributed to
384 improved fuel-air mixing. Advancing SoMI timing resulted in slightly higher cylinder
385 noise, however variation of SoPI timing didn't affect combustion noise. These results
386 showed that variations in SoI timings didn't affect knocking characteristics. Knocking

387 characteristics of PCCI combustion at different SoPI and SoMI timings showed that 35°
388 bTDC resulted in slightly stable combustion compared to relatively advanced (30° bTDC)
389 or retarded (40° bTDC) SoPI timings. This was mainly due to trade-off between in-
390 cylinder conditions and time availability for fuel-air mixing, which directly influenced
391 combustion phasing.

392 Figure 5 (b) shows the variations in KI, KP and combustion noise at different SoMI
393 timings and EGR rates. KI slightly decreased with advancing SoMI timings. Increasing
394 EGR reduced KI, which reflected smoother combustion at higher EGR rates. This
395 observation was further validated by KP results. As EGR rate increased from 0 to 30%,
396 KP decreased from ~8 to ~2 bar. This was mainly due to dilution effect of EGR, which
397 directly controlled the chemical kinetics of fuel-air mixture. At higher EGR rates, lower
398 in-cylinder temperatures also suppressed knocking. Cylinder noise was also significantly
399 affected by EGR. With increasing EGR rates from 0 to 30%, combustion noise
400 continuously decreased from ~98 to ~92 dB. Comparison of PCCI combustion results at
401 different EGR rates indicated that EGR played an important role in PCCI combustion
402 thus showing its potential for noise and knock reduction. However too high EGR
403 adversely affected the performance of PCCI engines and resulted in higher HC and CO
404 emissions.

405

406 **3.2 Performance Characteristics**

407 To investigate the effects of split injection and EGR on PCCI engine performance,
408 experiments were carried out at varying SoPI timings and EGR rates. In this study,
409 brake thermal efficiency (BTE), brake specific fuel consumption (BSFC) and exhaust gas
410 temperature (EGT) were measured and plotted w.r.t. SoMI timings. At each
411 experimental condition, performance parameters were measured three times and
412 average was presented with error bars.

413

414 Figure 6: Variations in BTE, BSFC and EGT w.r.t. SoMI timings at different (a) SoPI
415 timings and (b) EGR rates

416 Figure 6 (a) shows the variations in PCCI engine performance parameters at varying
417 SoPI and SoMI timings. Results obtained show that BTE decreased with advancing
418 SoMI timings. This was mainly due to dominant premixed combustion phase, which led
419 to relatively higher negative piston work, resulting in lower BTE. Advancing SoPI
420 timing from 30 to 35° bTDC resulted in slightly higher BTE, but further advancing SoPI
421 timing (up to 40° bTDC) decreased BTE drastically. With retarded SoPI timing (30°
422 bTDC), lesser time availability for fuel-air mixing led to inferior combustion. However
423 with advanced SoPI timing (40° bTDC), lower peak cylinder pressure and temperature
424 both dominated, resulting in inferior combustion. BSFC followed similar behavior at
425 different SoMI and SoPI timings, with lowest BSFC attained at intermediate SoPI (35°
426 bTDC) and retarded SOMI (12° bTDC) timing. EGT was measured very close to the
427 exhaust port. EGT gives qualitative information of in-cylinder combustion. In PCCI
428 combustion, EGT was observed to be significantly lower (~100°C) compared to CI
429 combustion [39] and was attributed to absence of diffusion combustion. Application of
430 EGR was another important reason for lower EGT in PCCI combustion mode. In this
431 study, EGT slightly reduced with advanced SoMI and SoPI timings. This was due to
432 longer time availability, which improved fuel-air mixing and promoted premixed
433 combustion. Negligible diffusion combustion with slightly lower EGT was observed.
434 Amongst the three SoPI timings, 35° bTDC showed minimum EGT (~225°C).

435 Figure 6 (b) shows variation in engine performance parameters at different SoMI
436 timings and EGR rates. BTE decreased with increasing EGR rate. This was mainly due
437 to two reasons: (i) lower fuel quantity at higher EGR rates, which retarded the chemical
438 kinetics of fuel-air mixture, resulting in slightly inferior combustion, and (ii) lower in-

439 cylinder temperature due to presence of higher heat capacity exhaust gas, which
440 encouraged incomplete combustion. These factors resulted in higher CO and HC
441 emissions and adversely affected PCCI engine performance. BSFC followed a similar
442 trend. BSFC continuously increased with increasing EGR rate. Effect of EGR was also
443 seen by variations in EGT. EGT drastically decreased (by up to 75°C) with increasing
444 EGR rate. This is the main advantage of PCCI combustion because lower EGT
445 represents absence of diffusion combustion phase because thermal NO_x formation takes
446 place during diffusion combustion phase. Engine performance results showed that
447 increasing EGR rate slightly decreased the PCCI engine performance however
448 significant reduction in EGT occurred at 15% EGR rate. This shows a trade-off between
449 reduction in BTE and EGT, therefore it can be considered as optimized EGR rate for
450 PCCI combustion in the present experiment.

451

452 3.3 Emission Characteristics

453 To compare the PCCI mode engine emission characteristics, CO, HC, NO_x and smoke
454 opacity were measured at different SoPI timings (30, 35 and 40° bTDC) and EGR rates
455 (0, 15 and 30%). CO, HC and NO_x emissions are presented as brake specific mass
456 emissions (g/kWh) and smoke opacity is measured in absolute units.

457 Figure 7: Variations in mass emissions of CO, HC, NO_x and smoke opacity w.r.t. SoMI
458 timings at different (a) SoPI timings and (b) EGR rates

459 Figure 7(a) shows variations in CO, HC and NO_x emissions, and smoke opacity w.r.t.
460 SoMI timings at different SoPI timings. In IC engines, CO and HC are formed mainly
461 due to incomplete combustion. Other researchers have also reported slightly higher CO
462 and HC emissions from PCCI combustion mode [23-25]. CO is an intermediate
463 combustion product, primarily formed due to incomplete oxidation of CO to CO₂, under
464 relatively lower in-cylinder temperature conditions. Advanced SoMI timings lead to

465 relatively lower CO emissions. Relatively advanced combustion phasing at advanced
466 SoMI timings was the main reason for this behavior. Results showed that CO emission
467 increased slightly in case of advancing the SoPI timing from 30 to 35° bTDC. At
468 advanced SoPI timings, improved fuel-air premixing prevented diffusion combustion,
469 leading to relatively lower in-cylinder temperature. With further advancing SoPI timing
470 from 35 to 40° bTDC, CO emission slightly decreased. This was attributed to slightly
471 inferior in-cylinder conditions, which promoted diffusion combustion therefore lower CO
472 emissions. Similar to CO emissions, HC emissions were also observed to be higher in
473 PCCI combustion mode. In IC engines, HC formation takes place due to three reasons:
474 (i) incomplete combustion (shorter combustion duration), (ii) trapped fuel droplets in
475 crevice volume (early injection at higher FIPs), and (iii) in-cylinder wall quenching
476 (lower in-cylinder temperature). Results obtained show that HC emissions increased
477 with advancing SOMI and SoPI timings. Advancing SoI timings result in homogeneous
478 fuel-air mixture, which promotes premixed combustion. This leads to lower in-cylinder
479 temperature and forms HCs due to incomplete combustion and wall quenching. With
480 advanced SoI timings, relatively larger fraction of fuel enters into the crevice volume
481 resulting in higher HC emissions. Fuel spray impingement at advanced SoI timings may
482 be another reason for higher HC emissions, wherein fuel spray comes in contact with
483 cold in-cylinder walls and combustion is quenched. Higher HC emissions also affect
484 combustion efficiency adversely, which in turn reduce overall thermal efficiency. Ultra-
485 low NO_x emission is the main advantage of PCCI combustion. NO_x formation mainly
486 occurs in diffusion combustion phase, where in-cylinder temperatures are too high. In
487 PCCI combustion, absence of a prominent diffusion combustion phase is the prime
488 reason for lower NO_x formation. NO_x emissions increased slightly with advanced SoMI
489 timings. Amongst all three SoPI timings, lowest NO_x was obtained for 35° bTDC. This
490 was the main reasons for selecting 35° bTDC as the optimum SoPI timing in further

491 experiments. Smoke opacity reflects qualitative pollutant level in the exhaust gas.
492 Lower smoke opacity is another advantage of PCCI combustion. Results showed that
493 smoke opacity decreased with advancing SoMI timings. Improved fuel-air mixing due to
494 longer time availability was the main reason. Advancing SoPI timing first reduced
495 smoke opacity, however too advanced SoPI timing resulted in slightly higher smoke
496 opacity. Higher smoke opacity at 40° bTDC SoPI timing can be correlated to higher HC
497 emissions. Higher HC emissions promoted more soot nuclei formation, which resulted in
498 higher smoke opacity. Lowest smoke opacity at 35° bTDC SoPI timing makes it the most
499 favorable condition for PCCI combustion mode.

500 Figure 7(b) shows the variation in CO, HC and NO_x emissions, and smoke opacity at
501 varying SoMI timings and EGR rates. Results obtained showed that CO and HC
502 emissions increased with increasing EGR rates. At higher EGR rate, in-cylinder
503 temperature became too low, which reduced oxidation of CO to CO₂, leading to higher
504 CO emissions. At 30% EGR rate, availability of oxygen further reduced, resulting in
505 increased CO emission. CO emission can also be related to the retarded combustion
506 phasing, which resulted in slower chemical kinetics of fuel-air mixture, inhibiting CO to
507 CO₂ conversion. With increasing EGR rate, in-cylinder temperature became too low to
508 oxidize the fuel completely which increased the unburned HC emissions. Combustion
509 temperature near the cylinder walls was even lower due to higher heat losses. Therefore
510 at locations in the vicinity of cylinder walls, combustion was either quenched or did not
511 occur at all, which further increased the HC emissions. NO_x formation was found to be
512 sensitive to EGR. With increasing EGR rate, NO_x emissions reduced continuously.
513 These observations were in agreement with that of variations in EGT (Figure 6(b)).
514 Increasing EGR rate from 0 to 15% resulted in ~60% reduction in NO_x emissions.
515 Further increase in EGR rate led to even lower NO_x emissions, but it also caused
516 inferior and erratic engine performance. Therefore 15% EGR rate was considered as a

517 reasonable trade-off between the engine performance and the emission characteristics.
518 Smoke opacity slightly increased with increasing EGR rate, which led to lower in-
519 cylinder temperatures. At higher EGR rate, lower in-cylinder temperatures promoted
520 soot formation and enhanced smoke opacity. Overall emission results reflected that
521 increasing EGR rate resulted in slightly higher CO, and HC emissions and smoke
522 opacity, and these increments were relatively lower at 15% EGR rate compared to 30%
523 EGR rate. Therefore 15% EGR was used for optimizing PCCI engine performance and
524 emission characteristics.

525

526 3.4 Particulate Characteristics

527 To compare the characteristics of particulate emitted by diesel fuelled PCCI engine, two
528 parameters used were: (i) Particulate number-size and (ii) Particulate surface area-size
529 distributions. Particulate number-size distribution was determined after thermal
530 stabilization of the engine. Particulate sampling was done for one minute at a sampling
531 frequency of 1 Hz. Average of these 60 data points were analyzed and presented along
532 with standard deviation as the error bars, in the following figures. Figure 8 shows the
533 number-size and surface area-size distributions of particulate at varying SoPI and SoMI
534 timings, and 15% EGR rate.

535 Figure 8: (a) Number-size and (b) Surface area-size distributions of particulate at
536 varying SoPI and SoMI timings, and 15% EGR rate

537 Variations in particulate number-size distributions with SoPI and SoMI timings can be
538 correlated with two parameters, namely (i) in-cylinder conditions (temperature and
539 pressure), and (ii) time availability (for fuel-air mixing). Trends clearly indicated that
540 particulate number concentration at a given size decreased with advancing SoMI
541 timings. This was mainly due to relatively longer time available for fuel-air mixing,
542 which resulted in formation of more homogeneous mixture. PCCI combustion at

543 advanced SoMI timings shifted peak particulate number-size distribution towards
544 larger particulate. This showed higher adsorption of condensed exhaust species on
545 primary particles. With advanced SoPI timing, particle number concentration first
546 decreased (from 30 to 35° bTDC) and then increased (from 35 to 40° bTDC). Advancing
547 SoPI timing from 30 to 35° bTDC decreased particulate number concentration, however
548 peak of particulate number size-distribution shifted towards larger particles. Effect of
549 variation of SoMI timing was also relatively more significant at 35° bTDC, which
550 resulted in slightly lower in-cylinder temperature due to improved fuel-air pre-mixing.
551 Lower in-cylinder temperature enhanced particulate agglomeration, leading to larger
552 particles in relatively lower concentration. At 30° bTDC SoPI timing, less time
553 difference between pilot injection and the main injection dominated over superior in-
554 cylinder conditions, which resulted in slightly inferior fuel-air mixing, leading to higher
555 particulate number concentration. However at 40° bTDC SoPI timing, relatively inferior
556 in-cylinder conditions dominated over longer time availability, leading to
557 inhomogeneous fuel-air mixing resulting in emission of higher number of particles. Due
558 to presence of inferior in-cylinder conditions, soot nuclei formation increased, resulting
559 in higher particulate number concentration, however longer time availability affected
560 particulate size. Too advanced SoPI timing (40° bTDC) improved fuel-air pre-mixing and
561 size of peak particulate number concentration decreased in comparison to intermediate
562 SoPI timing (35° bTDC). At 35° bTDC SoPI timing, particulate size distribution was
563 relatively wider in comparison to other SoPI timings. This indicated trade-off between
564 fuel-air pre-mixing time and in-cylinder conditions. In the experiment, 30° bTDC SoPI
565 showed maximum particle concentration (6×10^7 particles/cm³ exhaust gas) and 35°
566 bTDC SoPI showed minimum particle concentration (3×10^7 particles/cm³ exhaust gas).
567 Particulate surface area-size distribution affects the toxicity of particulate because
568 higher surface area of particulate increases probability of surface adsorption of toxic

569 gaseous species and PAHs. Particle surface area was calculated by assuming them to be
570 spherical.

$$571 \quad dS = dN.(D_p)^2$$

572 Here dS is the area concentration of the size range with mean diameter D_p and dN is the
573 number concentration of particles with mean diameter D_p . Higher number concentration
574 of smaller particles results in higher surface area in comparison to surface area of lower
575 number of larger particles. Smaller particles have the ability to penetrate deeper in the
576 respiratory system, which enhances the possibility of them causing several diseases [40].
577 Smaller particles also have longer retention time in the environment due to their lower
578 settling velocity. This increases their possibility to be inhaled in the human body.
579 Therefore smaller particles tend to become more hazardous for human health as
580 opposed to larger particles.

581 From figure 8(b), it can be observed that particle surface area distribution decreased
582 with advancing SoMI timing. This trend was common at all SoPI timings. With
583 advancing SoPI timings, particulate surface area decreased continuously with trend
584 slightly different from that of particle number-size distribution. Advancing SoPI timing
585 improved fuel-air pre-mixing, leading to lower particulate concentration. At too
586 advanced SoPI timing, particle number concentration increased slightly, however
587 particulate size distribution decreased. These two counter effects resulted in lower
588 particulate surface area. At too advanced SoPI timings (40° bTDC), wider particle
589 surface area-size distributions also showed the contribution of larger particles to the
590 total particulate surface area. This showed that contribution of larger particles ($D_p > 200$
591 nm) to the total particulate surface area was almost equal to the contribution of small
592 particles ($D_p < 200$ nm). Due to longer time availability for fuel-air premixing, variation
593 of SoMI timing was slightly less effective at advanced SoPI timings. Overall, the results
594 at different SoPI timings suggested that intermediate SoPI timing was suitable for

595 PCCI combustion because it resulted in larger particulates in lower number
596 concentration, which are less harmful to the human health.

597 Figure 9 (a) shows particle number-size distribution at varying EGR rates and SoMI
598 timings.

599 Figure 9: (a) Number-size and (b) surface area-size distributions of particulate at
600 varying EGR rates and SoMI timings

601 Similar to SoPI results, advancing SoMI timing resulted in lower particulate number
602 concentration however reduction at advanced SoMI timings was higher at 0 and 30%
603 EGR rates compared to 15% EGR rate. Figure 9(a) showed that the particle number
604 concentration first decreased with increasing EGR rate (up to 15%) and then increased
605 drastically with further increasing EGR rate up to 30%. There were two factors
606 responsible for this observation. First was the shifting of combustion phasing, which
607 improved combustion efficiency leading to lower number of soot nuclei formation. Second
608 factor was the dilution effect, which reduced in-cylinder temperature and increased
609 particulate formation near the cylinder walls (due to presence of fuel-rich pockets
610 formed during combustion quenching and spray impingement). When EGR rate
611 increased up to 15%, the first factor dominated, resulting in lesser particulate number
612 emissions. However at 30% EGR rate, second factor dominated, resulting in significantly
613 higher particulate number emissions. With increasing EGR rate, peak of particle
614 number-size distribution also shifted towards larger particles. This was mainly due to
615 lower in-cylinder temperatures at higher EGR rate, which promoted condensation of
616 volatile organic species. These condensates were adsorbed on to the primary particulate
617 surface, resulting in larger particles. Figure 9(b) shows that the particulate surface
618 area-size distribution followed similar trend as that of particulate number-size
619 distribution. With increasing EGR rate, particulate surface area increased due to
620 formation of larger particulate. At 30% EGR rate, peak of particulate surface area

621 significantly increased compared to 0 and 15% EGR rates. This was mainly due to
622 higher number concentrations of relatively smaller particles. Amongst all three EGR
623 conditions, 15% EGR rate was found to be most suitable for PCCI combustion mode
624 because of its lower particulate number as well as surface area distributions.

625 Overall analysis of particulate emitted from PCCI combustion mode was carried out in
626 terms of nucleation mode particles (NMP) ($D_p < 50$ nm) and accumulation mode particles
627 (AMP) ($50 \text{ nm} < D_p < 1000$ nm) concentrations; total particle number (TPN)
628 concentration and count mean diameter (CMD) (Figure 10). These parameters were
629 calculated from particulate number-size distributions. Figure 10(a) shows the analysis
630 of particulate emitted from PCCI combustion at different SoPI and SoMI timings. With
631 advanced SoMI timings, NMP concentration remained almost constant at 30° and 40°
632 bTDC SoMI timings, however it slightly decreased at 35° bTDC timing. This showed
633 that the formation of NMP was affected by two factors: (i) in-cylinder conditions, and (ii)
634 fuel-air pre-mixing time. At too advanced or retarded SoPI timings, one factor always
635 dominated, resulting in higher NMP. At intermediate SoPI timing, trade-off among
636 these two factors showed the effect of variations in SoMI timing, which increased the
637 fuel-air pre-mixing and resulted in lower NMP concentration. Amongst all three SoPI
638 timings, 35° bTDC resulted in lowest NMP concentration. At all SoPI timings, NMP
639 concentration was $> 1 \times 10^8$ particles/cm³ of exhaust gas, which was significantly lower
640 than HCCI combustion and conventional CI combustion modes [38]. With advanced
641 SoMI timing, AMP concentration slightly decreased due to improved fuel-air pre-mixing.
642 AMP concentration also followed similar trend as that of NMP. However AMP
643 concentration ($\sim 4 \times 10^8$ particles/cm³ of exhaust gas) was higher than NMP concentration
644 ($\sim 1 \times 10^8$ particles/cm³ of exhaust gas).

645 Figure 10: Number of Nucleation mode particles, number of accumulation mode
646 particles, total particulate number, and count mean diameter of particulate for varying
647 SoMI timings at different (a) SoPI timings and (b) EGR rates

648 Figure 10(a) shows that 30 and 35° bTDC SoPI timings showed the highest TPN
649 concentration ($\sim 5 \times 10^8$ to 6×10^8 particles/cm³ of the exhaust gas) and the lowest TPN
650 concentration ($\sim 3 \times 10^8$ to 4×10^8 particles/cm³ of exhaust gas) respectively. For all SoPI
651 timings, advancing SoMI timings resulted in relatively lower TPN concentration. At 24°
652 bTDC SoMI timing, reduction in TPN concentration was slightly lower due to inferior
653 in-cylinder conditions. Advancing SoPI timing also resulted in lower TPN concentration,
654 however too advanced SoPI timing led to slightly higher TPN concentration due to
655 inferior fuel vaporization in presence of lower in-cylinder temperatures. Average size of
656 particulate emitted at different SoPI and SoMI timings were presented by CMD. CMD
657 showed the number averaged diameter of particulate. Results showed that particulate
658 emitted at 35° bTDC SoPI timing had the highest CMD and particles emitted from 30°
659 bTDC SoPI timing had the lowest CMD. At 12° SoMI timing, CMD of particulate at
660 different SoPI timings was almost same. This was attributed to longer time difference
661 between SoPI and SoMI timings, which decreased with advancing SoMI timings. At 35°
662 and 40° SoPI timing, CMD increased with advancing SoMI timings, however CMD was
663 almost constant at 30° bTDC SoPI timing. CMD varied mainly due to variations in
664 particle number as well as particle size.

665 Figure 10(b) shows the variations in NMP, AMP and TPN concentrations, and CMD of
666 particulate emitted from PCCI combustion at different SoMI timings and EGR rates.
667 NMP concentration remained almost same at different EGR rates. With increasing EGR
668 rates, AMP concentration increased due to reduction in peak cylinder temperature and
669 chemical kinetics of fuel-air mixtures. These two factors promoted formation of higher
670 number of soot nuclei as well as particulate agglomeration. At 15% EGR rate, AMP

671 concentration remained almost constant, however at 30% EGR rate, AMP concentration
672 increased drastically. At 15% EGR rate, particulate number concentration decreased
673 due to slightly improved combustion phasing. At 30% EGR rate, too retarded
674 combustion phasing resulted in emission of large number of particulate. TPN trends
675 showed that 30% EGR rate resulted in maximum TPN concentration ($\sim 7 \times 10^8$
676 particles/cm³ of exhaust gas) and 15% EGR rate resulted in minimum total particle
677 concentration ($\sim 3 \times 10^8$ particles/cm³ of exhaust gas). Advancement of SoMI timing led to
678 lower TPN concentration. Variations in CMD of particulate showed that 30% EGR rate
679 resulted in formation of larger particles compared to 0% and 15% EGR rates. Increasing
680 EGR rate enhanced condensation of volatile species due to lower in-cylinder
681 temperatures. These condensates were adsorbed on to primary particulates, which
682 increased the particulate size, leading to higher CMD.

683 Particulate analysis showed that 35° bTDC SoPI timing was most suitable for PCCI
684 combustion mode. At 35° bTDC SoPI timing, TPN concentration was lowest with the
685 highest CMD, which reduced their potential harmful effects. Comparison of particulate
686 emission characteristics at different EGR rates showed slight reduction in particulate
687 number concentration at 15% EGR rate and significantly higher particulate number
688 concentration at 30% EGR rate. Therefore 15% EGR rate was suitable for PCCI
689 combustion.

690 **3.5 Particulate Bound Trace Metals**

691 For detailed particulate analysis, particulate samples were analyzed for trace metals.
692 The experiments were carried out in two stages. In the first stage, effect of SoPI timings
693 was investigated by analyzing three particulate samples collected at SoPI timings of 30,
694 35 and 40° bTDC. In the second stage, effect of EGR was investigated by analyzing three
695 particulate samples collected at EGR rates of 0, 15 and 30%. During these experiments,
696 all other parameters such as SoMI and FIP were maintained constant at 16° and 700

697 bar respectively. In trace metal analysis, total of 34 trace metals were detected in the
698 particulate samples, however only 20 trace metals, which could be detected with <90%
699 accuracy level are discussed here. These trace metals were further classified into five
700 groups based on their origin, their health effects and for convenience of presentation
701 (figure 11).

702 Figure 11: Particulate bound trace metals at different (a) SoPI timings and (b) EGR
703 rates

704 Figure 11 shows particulate bound trace metals emitted from the engine at different
705 SoPI timings and EGR rates during PCCI combustion mode. First group contained
706 traces of Al, Cu, Fe and Zn, which are harmful for human health due to their reactive
707 oxygen species (ROS) generation potential, and can lead to onset of cancer. Main source
708 of these trace metals are the wear debris of engine components. These wear debris are
709 picked up by the lubricating oil, which is recirculated in an engine in order to reduce
710 friction between piston rings and cylinder liner interface. During combustion, pyrolysis
711 of lubricating oil also contributes to these trace metals in the particulate. Zinc
712 containing compounds are commonly used as additives in lubricating oils and greases.
713 During combustion, these compounds undergo thermo-oxidative decomposition in
714 presence of oxygen to form zinc poly phosphate, which gets converted into ZnO and
715 emitted as trace metal. At advanced SoPI timings, improved fuel-air mixing resulted in
716 lower particulate emissions with consequently lower trace metal content. Increasing
717 EGR rate showed significant reduction in concentration of these trace metals in the
718 particulate. At higher EGR rate, lower in-cylinder temperatures reduced pyrolysis of
719 lubricating oil, leading to lower emissions of these trace metals, which is different from
720 HCCI combustion trace metals emission characteristics [28]. Results showed that the
721 concentration of Al and Fe traces decreased with advancing SoPI timings, however Cu
722 and Zn trace concentrations slightly increased at 35° bTDC SoPI timing. In this group,

723 Al concentration was relatively higher (~8 to 10 ppm/mg of PM) compared to other trace
724 metals. Second group of trace metals included Ca, K, Na and Mg. Pyrolysis of
725 lubricating oil was the main source of these metals. These trace metals are a part of
726 different organo-metallic additives added to the lubricating oil in order to improve its
727 lubricity, corrosion resistance, etc. Concentrations of these trace metals were slightly
728 higher in PCCI combustion mode. These trace metals do not affect human health
729 therefore these trace metals were not much discussed in previous studies [28, 41].
730 Advancing SoPI timings didn't show significant variation in concentration of these trace
731 metals. Results showed that trace concentrations of Ca, Na and Mg decreased with
732 increasing EGR rate since lower in-cylinder temperatures reduced pyrolysis of
733 lubricating oil. The third group of trace metals included Ni, Cr, Cd and As, which
734 primarily originate from wear of metallic engine components and lubricating oil
735 additives. These metals are not harmful in their pure form however they easily combine
736 with other species to form highly toxic compounds. Lower concentration of Ni, Cd and As
737 was due to relatively lower in-cylinder temperature during PCCI combustion mode.
738 Nickel is used as an additive in the lubricating oil in very small concentration as Nickel
739 ethoxy-ethyl-xanthate for improving lubrication quality. Upon combustion, these
740 compounds dissociate to release nickel, which reacts with sulphur and forms a
741 carcinogenic compound NiS [42]. Concentration of Ni emitted from PCCI engine was
742 significantly lower compared to HCCI engine, which was mainly due to lower particulate
743 emission (Figure 8) [28]. In the experiments, Cr was found to be in relatively higher
744 concentration and its trace concentration decreased with advanced SoPI timing and
745 increasing EGR rate. This trend is different from gasoline fuelled HCCI combustion in
746 which Cr concentration slightly increased with increasing EGR rate [41]. Fourth group
747 of trace metals included Pb, Mo, Sr and Ba, which primarily originate from fuel,
748 lubricating oil and sometimes from wear of engine components such as gaskets, piston

749 rings, etc. Pb, Mo, Sr and Ba are also harmful for human health. These trace metals
750 didn't show any specific trend in variation with SoPI timings. Pb, Mo and Sr
751 concentrations decreased with increasing EGR rate. Lower in-cylinder temperatures at
752 higher EGR rates were the main reason for this trend, which reduced the deterioration
753 of softer engine components such as gaskets and seals. However Pb, Sr and Ba were
754 lowest for 15% EGR rate. Last group of trace metals included Mn, Bi, In and V, which
755 are generally used in engine components to enhance their properties. Therefore wear of
756 engine components was the main source of these metal traces. Concentration of these
757 trace metals were found to be very low, which didn't show any specific trend at different
758 SoPI timing and EGR rate.

759 Comparison of trace metals emitted from PCCI combustion and HCCI combustion shows
760 one important finding that concentration of harmful trace metals were significantly
761 lower in PCCI combustion mode [28]. This was attributed to lower particulate emissions
762 from PCCI combustion mode. Therefore this study clearly indicates that optimized PCCI
763 combustion is beneficial for particulate reduction compared to HCCI combustion.

764

765 **3.5 Statistical Analysis**

766 To compare different split injection strategies and EGR rates, statistical analysis of PM
767 mass and NO_x emissions was plotted. This analysis gave a direct comparison of
768 effectiveness of combustion at different fuel injection strategies and EGR rates. Height
769 of rectangle showed particulate mass and width of the rectangle represented NO_x
770 emission. Area of the rectangle represented the combined emission of PM and NO_x.
771 Overall objective of this study was to reduce the area under the curve.

772 Figure 12: NO_x-PM mass analysis at varying (a) SoPI timings and (b) EGR rates in
773 PCCI combustion mode

774

775 Figure 12 (a) shows the variation of brake specific NO_x (BSNO_x) with PM mass
776 emissions at different SoMI and SoPI timings. In all cases, it was observed that
777 advancing SoMI timings resulted in higher NO_x but lower PM emissions. This was
778 attributed to longer time availability for fuel-air mixing, which resulted in superior
779 combustion and led to slightly higher NO_x emission. For a particular SoMI timing,
780 advancement in SoPI timing from 30 to 35° bTDC resulted in simultaneous reduction in
781 PM and NO_x. However further advancement in SoPI timing led to lower PM (due to
782 more time available for fuel-air pre-mixing) but higher NO_x emissions. Due to slightly
783 inferior cylinder conditions, performance and combustion also degraded at 40° bTDC
784 compared to 35° bTDC. PM and NO_x emission showed an interesting behavior with the
785 EGR rate (Figure 12(b)). An increment in EGR rate from 0 to 15% simultaneously
786 reduced NO_x and PM emissions. NO_x emissions reduced primarily due to lower in-
787 cylinder temperatures. An increase in EGR rate led to slower chemical kinetics of fuel-
788 air mixtures, which resulted in slightly retarded combustion phasing. Retarded
789 combustion phasing increased overall combustion duration, which provided sufficient
790 time for soot oxidation, led to relatively lower PM emission. However 30% EGR led to
791 very low combustion temperature, which reduced NO_x emissions significantly. However
792 incomplete combustion resulted in drastically higher PM emissions. Poor engine
793 performance and higher PM emission at 30% EGR made it unsuitable for PCCI
794 combustion mode. Therefore, 15% EGR rate and 35° bTDC SoPI timing were found to be
795 the most suitable conditions for PCCI combustion mode in a medium-duty diesel engine.

796

797 **Conclusions**

798 This experimental study was carried out to investigate suitable split injection
799 parameters and EGR rate for optimized PCCI combustion. The experiments were
800 carried out at different SoMI timings (12 to 24° bTDC), SoPI timings (30 to 40° bTDC)

801 and EGR rates (0, 15 and 30%). During the experiment, FIP was maintained constant at
802 700 bar. Results showed that advancing SoMI and SoPI timings improved PCCI
803 combustion, but too advanced SoPI timings resulted in slightly inferior performance and
804 emission characteristics. Advancing SoPI from 30 to 35° bTDC improved chemical
805 kinetics of fuel-air mixture and led to slightly higher P_{max} and highest HRR. At 40° SoPI
806 timing, combustion degraded slightly due to inferior combustion chamber conditions.
807 SoPI timing didn't show any significant effect of the SoC and combustion phasing.
808 Advancing SoPI timing reduced knocking and resulted in lower knock peak and
809 combustion noise. BTE improved slightly at SoPI timing of 35° bTDC however it
810 drastically reduced at SoPI timing of 40° bTDC. EGT also showed that intermediate
811 SoPI timing was suitable for PCCI combustion. NO_x, and smoke opacity were slightly
812 lower at SoPI timing of 35° bTDC. Particulate number concentration was the minimum
813 and average particulate size was the maximum at this condition as well. Particulate
814 bound trace metals didn't show any significant variation with changing SoPI timings.
815 Statistical analysis showed that advanced SoPI timing reduced PM mass and NO_x
816 emissions simultaneously, however too advanced SoPI timing led to slightly higher NO_x
817 emissions. Increasing EGR rate effectively controlled the HRR during PCCI combustion
818 mode, but very high EGR rate resulted in ultra-dilution of the combustible charge. This
819 led to very low peak in-cylinder temperature, resulting in very low BTE and higher HC
820 and CO emissions. Increasing EGR rate reduced the knocking and combustion noise
821 though. With higher EGR rate, NO_x emission decreased but PM mass emission
822 increased significantly. Trace metal analysis revealed that PCCI combustion emitted
823 relatively lower trace metals compared to HCCI combustion and concentration of most of
824 the reported trace metals decreased with increasing EGR rate. Overall effectiveness of
825 EGR on PCCI combustion mode was indicated by the statistical analysis. With
826 increasing EGR rate, NO_x and PM mass emission decreased simultaneously however

827 too high an EGR rate led to significantly higher PM mass emission. Therefore, it can be
828 concluded that optimum SoI timings and EGR rate can effectively control and enhance
829 engine performance and reduce emissions further in the PCCI combustion mode.

830

831 **Acknowledgements**

832 Authors are grateful to Technology Systems Group, Department of Science and
833 Technology (DST), Government of India for providing financial support (Grant no. DST/
834 TSG/ AF/ 2011/ 144-G dated 14-01-2013) for carrying out this experimental study.
835 Financial support from Council for Scientific and Industrial Research (CSIR),
836 Government of India's SRA scheme to Sh. Akhilendra Pratap Singh is also
837 acknowledged, which enabled his stay at ERL, IIT Kanpur for conducting the
838 experiments.

839

840 **References**

- 841 1. Akihama, K., Takatori, Y., Inagaki, K., Sasaki, S., Dean, A. M. (2001). Mechanism
842 of the smokeless rich diesel combustion by reducing temperature. SAE Technical
843 Paper 2001-01-0655.
- 844 2. Onishi, S., Jo, S. H., Shoda, K., Do Jo, P., Kato, S. (1979). Active thermo-atmosphere
845 combustion (ATAC)-a new combustion process for internal combustion engines. SAE
846 Technical Paper 790501.
- 847 3. Thring, R. H. (1989). Homogeneous-charge compression-ignition (HCCI) engines.
848 SAE Technical paper 892068.
- 849 4. Christensen, M., Johansson, B., Einewall, P. (1997). Homogeneous charge
850 compression ignition (HCCI) using isooctane, ethanol and natural gas-a comparison
851 with spark ignition operation. SAE Technical Paper 972874.

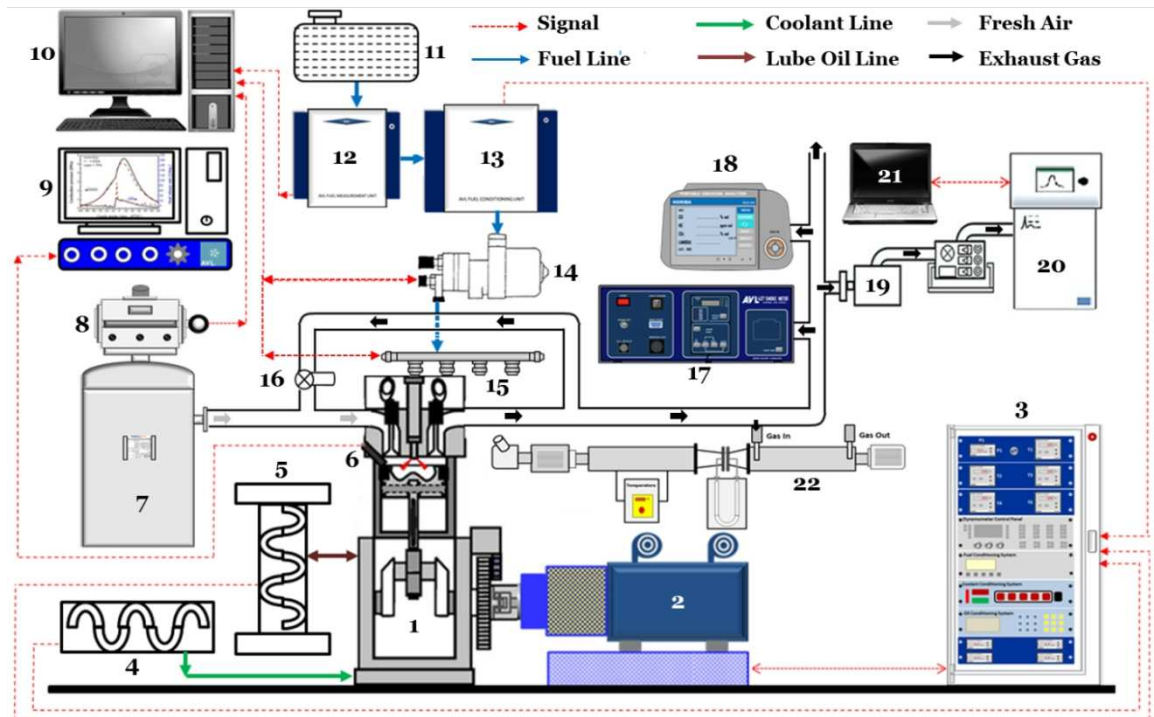
- 852 5. Stanglmaier, R. H., Roberts, C. E. (1999). Homogeneous charge compression
853 ignition (HCCI): benefits, compromises, and future engine applications. SAE
854 Technical Paper 1999-01-3682.
- 855 6. Maurya, R. K., Agarwal, A. K. (2011). Experimental investigation on the effect of
856 intake air temperature and air–fuel ratio on cycle-to-cycle variations of HCCI
857 combustion and performance parameters. *Applied Energy*, 88(4), 1153-1163.
- 858 7. Singh, A. P., Agarwal, A. K. (2012). Combustion characteristics of diesel HCCI
859 engine: an experimental investigation using external mixture formation technique.
860 *Applied Energy*, 99, 116-125.
- 861 8. Singh, A. P., Agarwal, A. K. (2012). An experimental investigation of combustion,
862 emissions and performance of a diesel fuelled HCCI engine. SAE Technical Paper
863 2012-28-0005.
- 864 9. Akagawa, H., Miyamoto, T., Harada, A., Sasaki, S., Shimazaki, N., and Hashizume,
865 T. (1999). Approaches to solve problems of the premixed lean diesel combustion.
866 SAE Technical Paper 1999-01-0183.
- 867 10. Hasegawa, R. and Yanagihara, H. (2003). HCCI combustion in DI diesel engine.
868 SAE Technical Paper 2003-01-0745.
- 869 11. Kimura, S., Aoki, O., Ogawa, H., Muranaka, S., and Enomoto, Y. (1999). New
870 combustion concept for ultra-clean and high-efficiency small DI diesel engines. SAE
871 Technical Paper 1999-01-3681.
- 872 12. Shimazaki, N., Tsurushima, T., and Nishimura, T. (2003). Dual-mode combustion
873 concept with premixed diesel combustion by direct injection near top dead center.
874 SAE Technical Paper 2003-01-0742.
- 875 13. Agarwal, A. K., Dhar, A., Srivastava, D. K., Maurya, R. K., Singh, A. P. (2014).
876 Effect of fuel injection pressure on diesel particulate size and number distribution
877 in a CRDI single cylinder research engine. *Fuel*, 107, 84-89.

- 878 14. Hashizume, T., Miyamoto, T., Akagawa, H., et al. (1998). Combustion and emission
879 characteristics of multiple stage diesel combustion. SAE Technical Paper 980505.
- 880 15. Neely, G. D., Sasaki, S., & Leet, J. A. (2004). Experimental investigation of PCCI-DI
881 combustion on emissions in a light-duty diesel engine. SAE transactions, 113(4),
882 197-207.
- 883 16. Horibe, N., Harada, S., Ishiyama, T., & Shioji, M. (2009). Improvement of premixed
884 charge compression ignition-based combustion by two-stage injection. International
885 Journal of Engine Research, 10(2), 71-80.
- 886 17. Torregrosa, A. J., Broatch, A., García, A., & Mónico, L. F. (2013). Sensitivity of
887 combustion noise and NO_x and soot emissions to pilot injection in PCCI Diesel
888 engines. Applied Energy, 104, 149-157.
- 889 18. Al-Qurashi, K., Boehman, A. L. (2008). Impact of exhaust gas recirculation (EGR)
890 on the oxidative reactivity of diesel engine soot. Combustion and Flame, 155,
891 675–695.
- 892 19. Kook, S., Bae, C., Miles, P., Choi, D., & Pickett, L. M. (2005). The influence of
893 charge dilution and injection timing on low-temperature diesel combustion and
894 emissions. SAE Technical Paper, 2, 005-01.
- 895 20. Kanda, T., Hakozaki, T., Uchimoto, T., Hatano, J., Kitayama, N., & Sono, H. (2005).
896 PCCI operation with early injection of conventional diesel fuel. SAE transactions,
897 114(3), 584-593.
- 898 21. Manente, V., Johansson, B., Tunestal, P. (2010). Characterization of partially
899 premixed combustion with ethanol: EGR sweeps, low and maximum loads. J. Eng.
900 Gas Turbines Power, 132, 082802.
- 901 22. Kiplimo, R., Tomita, E., Kawahara, N., & Yokobe, S. (2012). Effects of spray
902 impingement, injection parameters, and EGR on the combustion and emission
903 characteristics of a PCCI diesel engine. Applied Thermal Engineering, 37, 165-175.

- 904 23. André, M., Walter, B., Bruneaux, G., Foucher, F., & Mounaïm-Rousselle, C. (2012).
905 Exhaust gas recirculation stratification to control diesel homogeneous charge
906 compression ignition combustion. *International Journal of Engine Research*,
907 1468087412438338.
- 908 24. Jacobs, T., Bohac, S., Assanis, D. N., & Szymkowicz, P. G. (2005). Lean and rich
909 premixed compression ignition combustion in a light-duty diesel engine. SAE Paper
910 2005-01-0166.
- 911 25. Hardy, W. L., & Reitz, R. D. (2006). A study of the effects of high EGR, high
912 equivalence ratio, and mixing time on emissions levels in a heavy-duty diesel engine
913 for PCCI combustion SAE Technical Paper 2006-01-0026.
- 914 26. Price, P., Stone, R., Misztal, J., Xu, H., Wyszynski, M., Wilson, T., & Qiao, J. (2007).
915 Particulate emissions from a gasoline homogeneous charge compression ignition
916 engine. SAE Technical Paper 2007-01-0209.
- 917 27. Kittelson, D. B., & Franklin, L. (2010). Nanoparticle emissions from an ethanol
918 fueled HCCI engine. In Center for Diesel Research Department of Mechanical
919 Engineering University of Minnesota, Presented at Cambridge particle meeting.
- 920 28. Agarwal, A. K., Singh, A. P., Lukose, J., & Gupta, T. (2013). Characterization of
921 exhaust particulates from diesel fueled homogenous charge compression ignition
922 combustion engine. *Journal of Aerosol Science*, 58, 71-85.
- 923 29. Desantes, J., Benajes, J., García-Oliver, J. M., & Kolodziej, C. P. (2013). Effects of
924 Intake Pressure on Particle Size and Number Emissions from Premixed Diesel Low
925 Temperature Combustion. *International Journal of Engine Research*,
926 1468087412469514.
- 927 30. Abdul-Khalek, I., Kittleson, D., and Brear, F. (1999). The influence of dilution
928 conditions on diesel exhaust particle size distribution measurements. SAE
929 Technical Paper 1999-01-1142, 1999.

- 930 31. Idicheria, C. A., & Pickett, L. M. (2005). Soot formation in diesel combustion under
931 high-EGR conditions Sandia National Laboratories SAND2005-2879C.
- 932 32. Springer, K. J., 1997. Characterization of Sulfate, Odor, Smoke, POM and
933 Particulates from Light Duty and Heavy-duty Diesel Engines, Part IX. Prepared by
934 South West Research Institute.
- 935 33. Zhao, Y., Wang, Y., Li, D., Lei, X., & Liu, S. (2014). Combustion and emission
936 characteristics of a DME (dimethyl ether)-diesel dual fuel premixed charge
937 compression ignition engine with EGR (exhaust gas recirculation). *Energy*, 72, 608-
938 617.
- 939 34. Suh, H. K., Roh, H. G., Lee, C. S. (2008). Spray and combustion characteristics of
940 biodiesel/diesel blended fuel in a direct injection common-rail diesel engine. *Journal*
941 *of Engineering for Gas Turbines and Power*, 130, 032807.
- 942 35. Ganesh, V., Deshpande, S., & Sreedhara, S. (2015). Numerical investigation of late
943 injection strategy to achieve premixed charge compression ignition mode of
944 operation. *International Journal of Engine Research*. doi:
945 10.1177/1468087415585466
- 946 36. Rassweiler, G., Withrow, L. (1938). Motion Pictures of Engine Flames Correlated
947 with Pressure Cars. SAE Technical Paper 380139.
- 948 37. Singh, G., Singh, A. P., & Agarwal, A. K. (2014). Experimental investigations of
949 combustion, performance and emission characterization of biodiesel fuelled HCCI
950 engine using external mixture formation technique. *Sustainable Energy*
951 *Technologies and Assessments*, 6, 116-128.
- 952 38. Singh, A. P., Agarwal, A. K. (2016). Diesoline, Diesohol and Diesosene Fuelled
953 HCCI Engine Development. *Journal of Energy Resources Technology*, 138(5),
954 052212.

- 955 39. Agarwal, A. K., Srivastava, D. K., Dhar, A., Maurya, R. K., Shukla, P. C., Singh A.
956 P. (2013). Effect of fuel injection timing and pressure on combustion, emissions and
957 performance characteristics of a single cylinder diesel engine. *Fuel*; 111, 374-83.
- 958 40. McClellan, R.O. (1987). Health effects of exposure to diesel exhaust particles.
959 *Annual review of Pharmacology and Toxicology*, 27, 279-300.
- 960 41. Agarwal A. K., Lukose J., Singh A. P., Gupta T. (2015). Engine exhaust particulate
961 characterization of gasoline homogeneous charge compression ignition engine.
962 *Aerosol and Air Quality Research*; 15 (2), 504-516.
- 963 42. Sunderman Jr, F. W. (1978). Carcinogenic effects of metals. *Fed. Proc.*; (United
964 States) 37, no. 1.
- 965



966

967

968

969

970

971

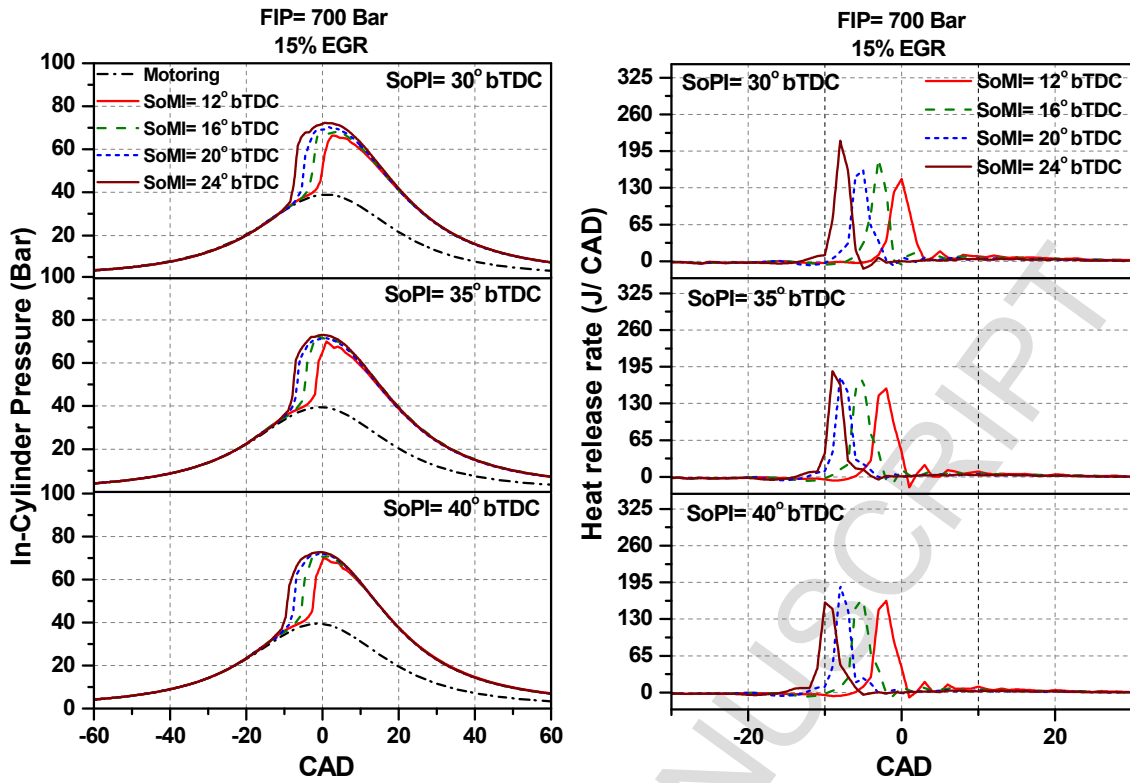
972

973

974

1- Single cylinder research engine, 2- Transient dynamometer, 3- Dynamometer controller, 4- Coolant conditioning system, 5- Lubricating oil conditioning system, 6- Pressure transducer, 7- Intake air surge tank, 8- Air-flow rate measurement system, 9- Combustion data acquisition system, 10- ECU interface system, 11- Fuel tank, 12- Fuel measurement system, 13- Fuel conditioning system, 14- High pressure fuel pump, 15- Common rail, 16- EGR valve, 17- Smoke opacimeter, 18- Exhaust gas emission analyzer, 19- Thermo diluter, 20- Engine exhaust particle sizer, 21- EEPS data logger, 22- Partial flow dilution tunnel

Figure 1: Schematic of the experimental setup



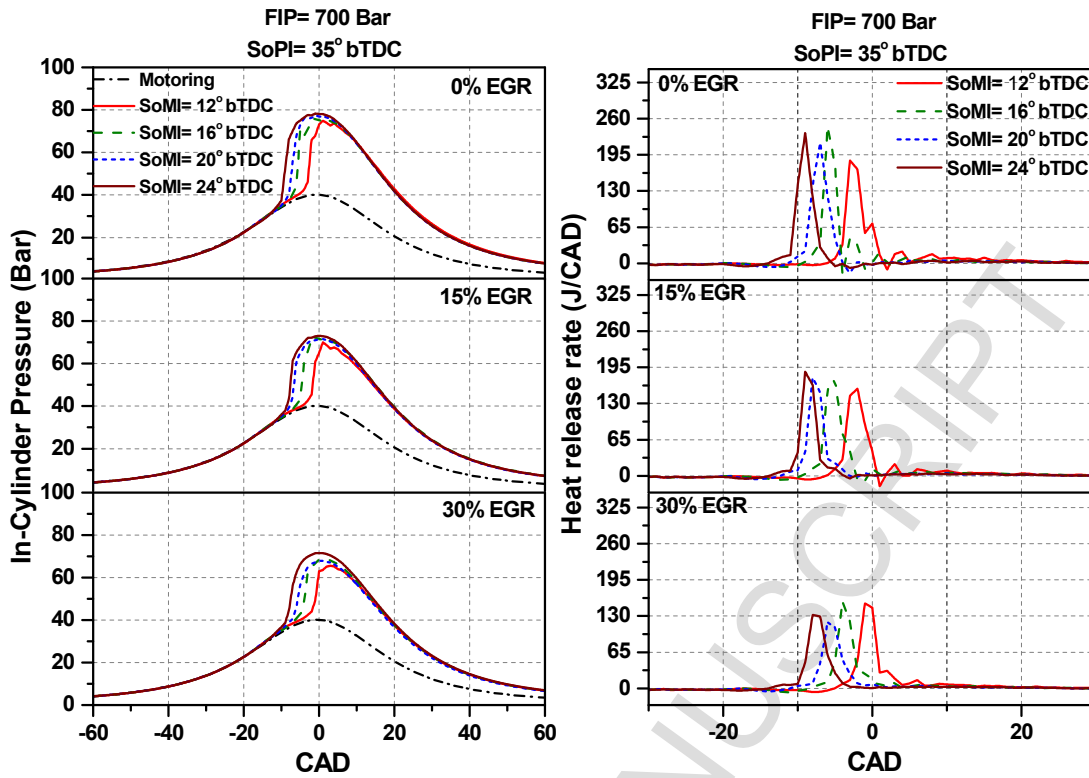
975

976 Figure 2: Variations in cylinder pressure and HRR w.r.t. crank angle at different SoPI

977

and SoMI timings

978



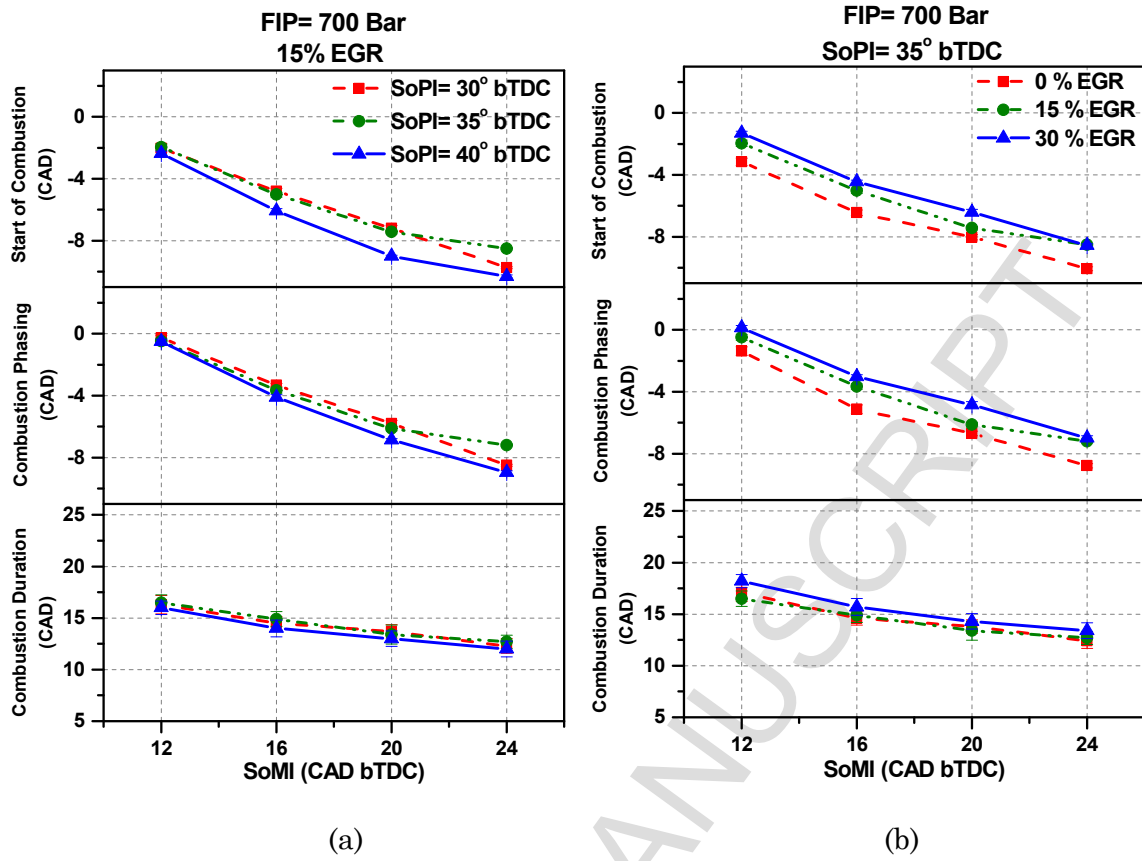
979

980 Figure 3: Variation in cylinder pressure and HRR w.r.t. crank angle for different SoMI

981

timings and EGR rates

982



983

984

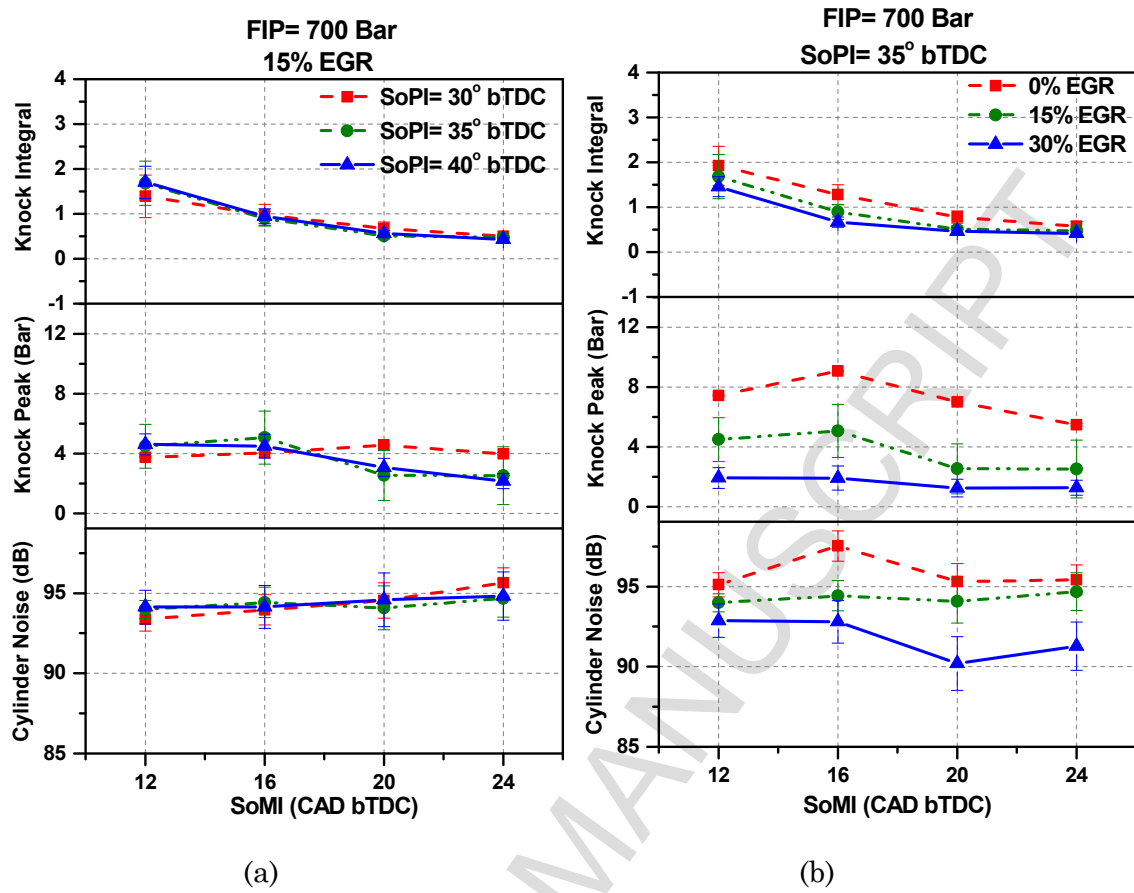
985

Figure 4: SoC, combustion phasing and combustion duration w.r.t. SoMI timings at different (a) SoPI timings and (b) EGR rates

986

987

988



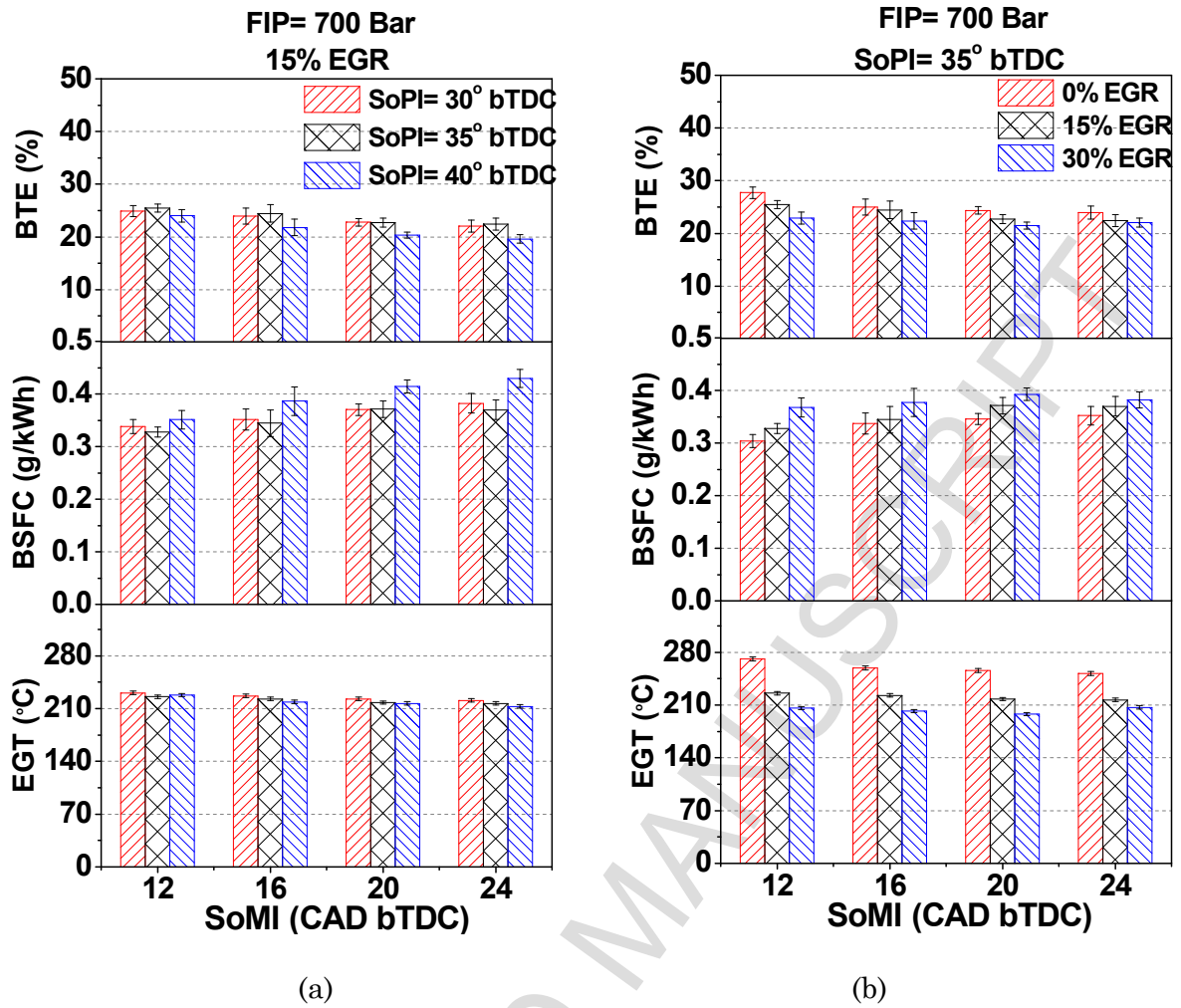
989

990

991

992

Figure 5: Variation in knock integral, knock peak and combustion noise w.r.t. SoMI timings at different (a) SoPI timings and (b) EGR rates



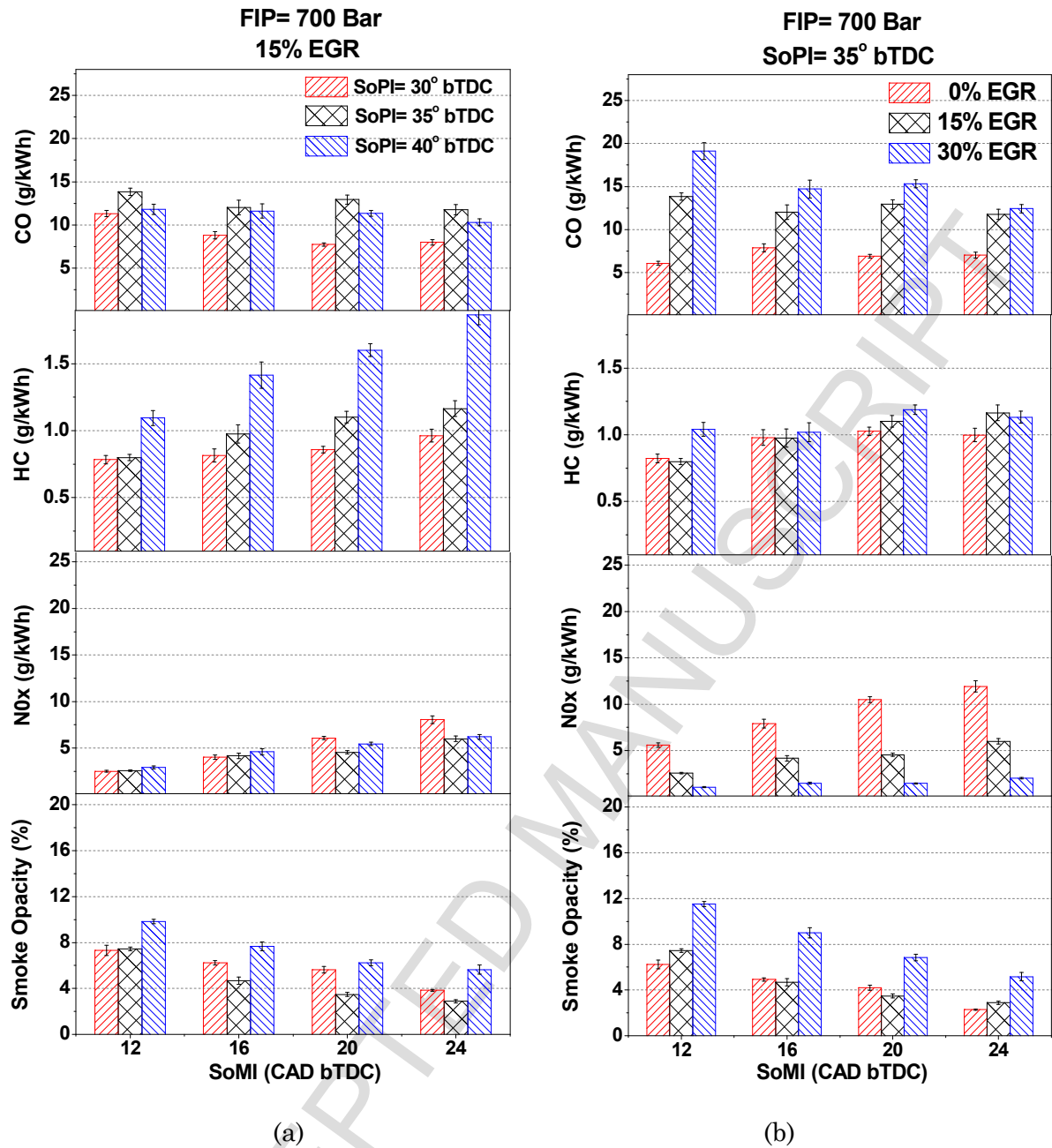
993

994

995

996

Figure 6: Variations in BTE, BSFC and EGT w.r.t. SoMI timings at different (a) SoPI timings and (b) EGR rates



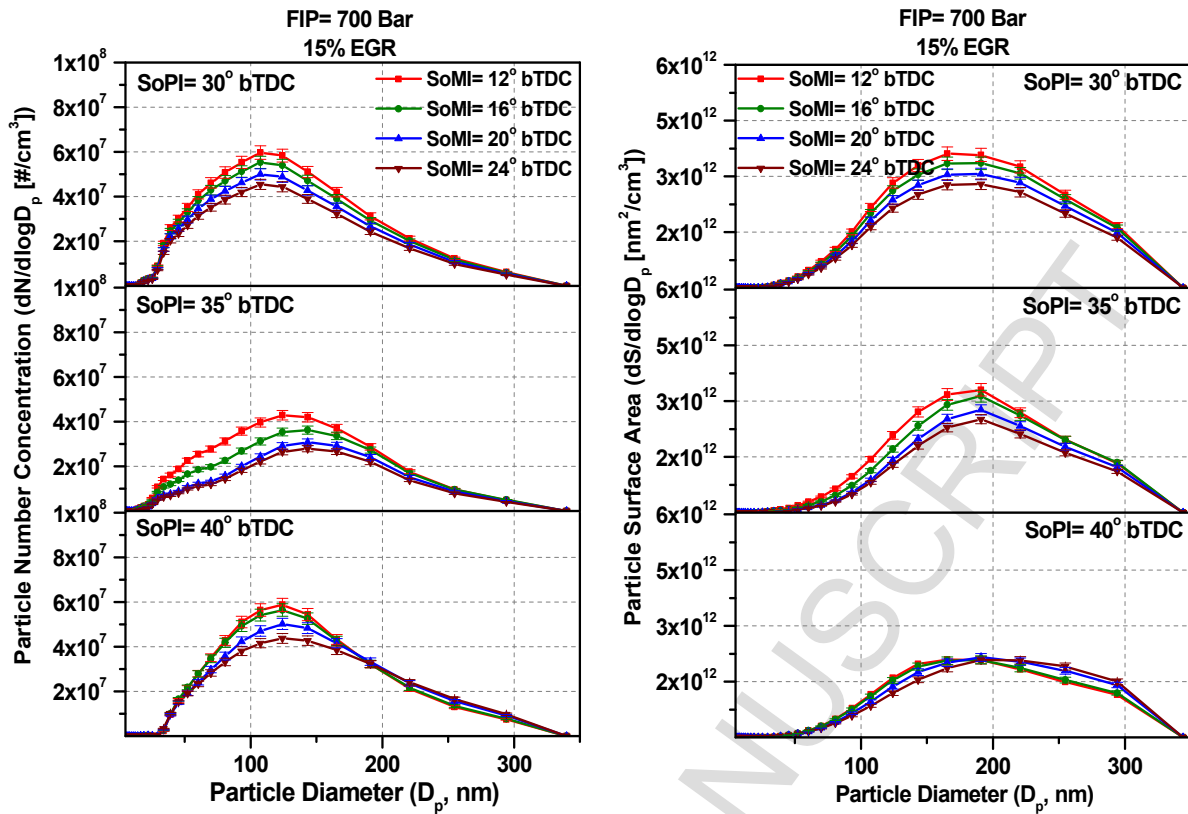
997

998

999

1000

Figure 7: Variations in mass emissions of CO, HC, NO_x and smoke opacity w.r.t. SoMI timings at different (a) SoPI timings and (b) EGR rates



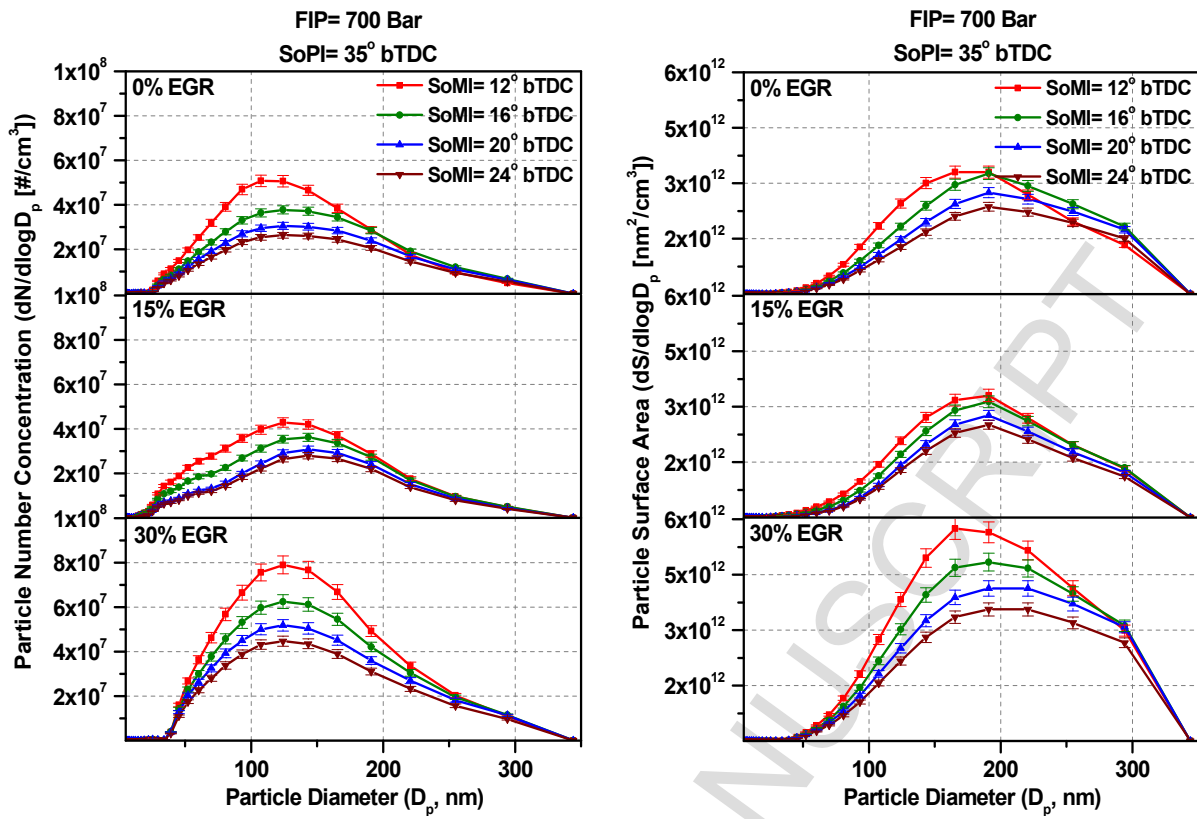
1001

1002

1003

1004

Figure 8: (a) Number-size and (b) Surface area-size distributions of particulate at varying SoPI and SoMI timings, and 15% EGR rate



1005

1006

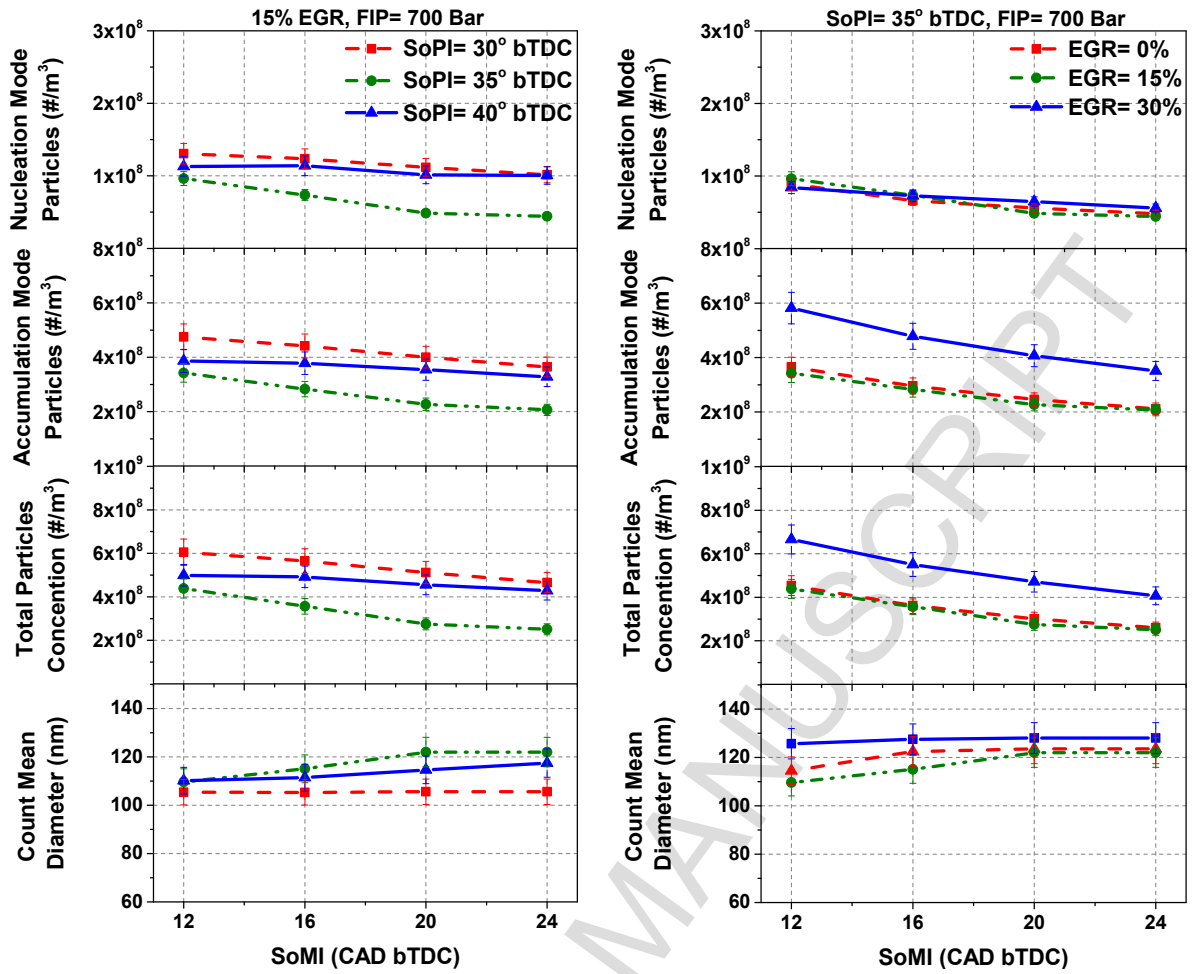
1007

1008

(a)

(b)

Figure 9: (a) Number-size and (b) surface area-size distributions of particulate at varying EGR rates and SoMI timings



1009

(a)

(b)

1010

1011

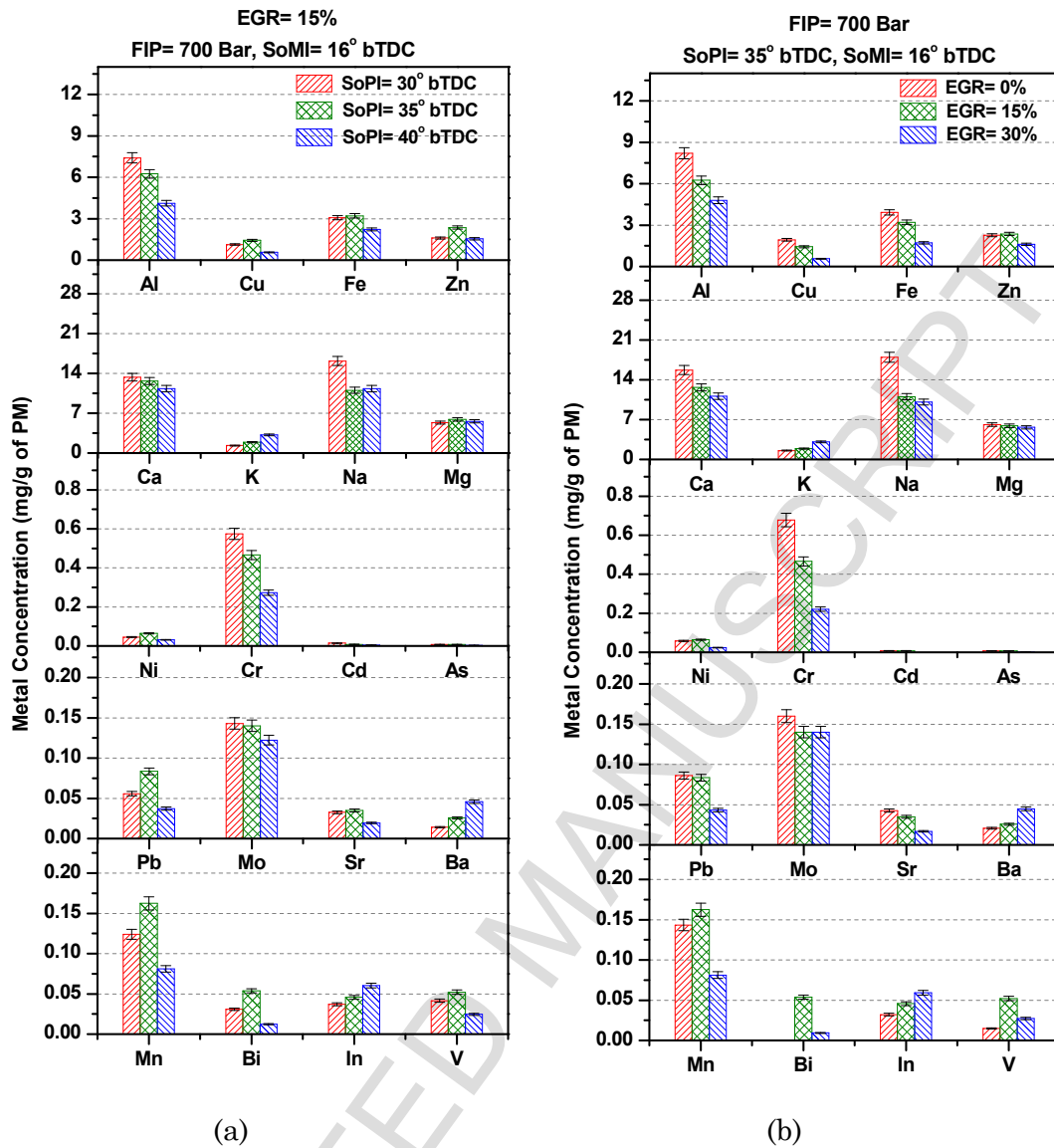
Figure 10: Number of Nucleation mode particles, number of accumulation mode

1012

particles, total particulate number, and count mean diameter of particulate for varying

1013

SoMI timings at different (a) SoPI timings and (b) EGR rates



1014

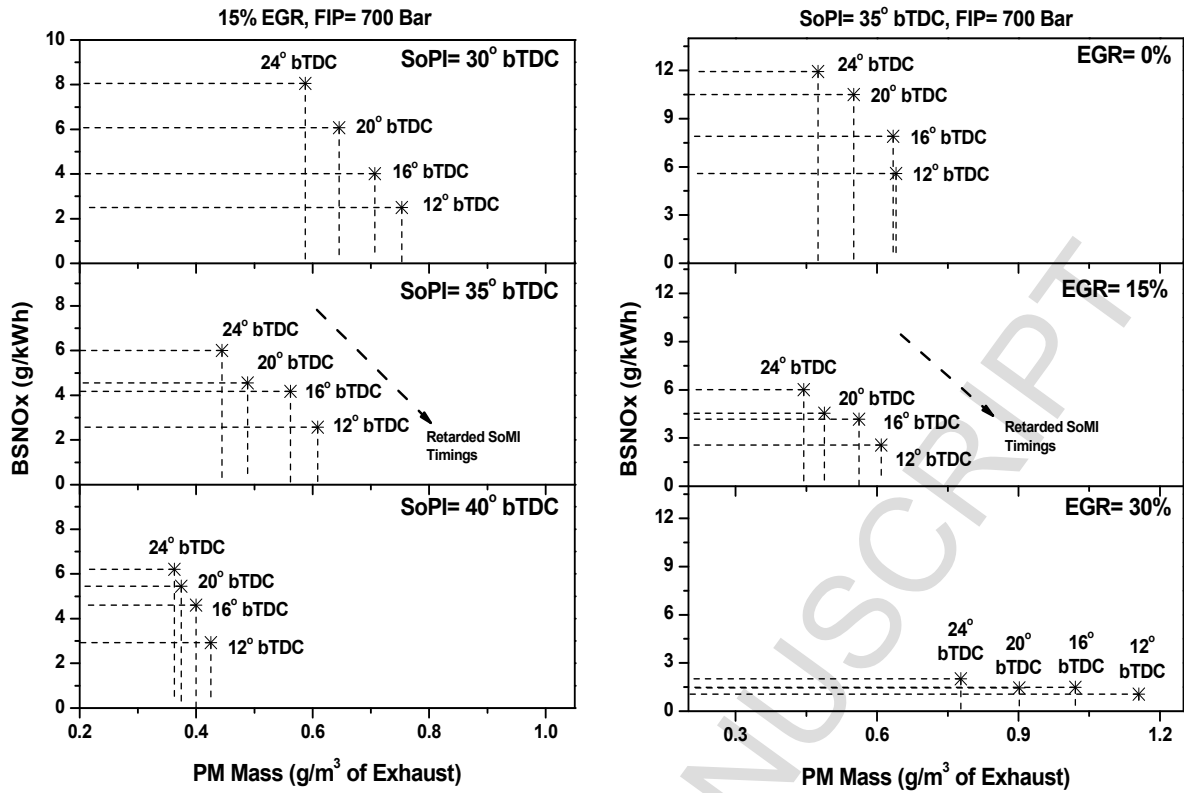
1015

1016

Figure 11: Particulate bound trace metals at different (a) SoPI timings and (b) EGR

1017

rates



1018

1019

1020

1021

1022

Figure 12: NO_x-PM mass analysis at varying (a) SoPI timings and (b) EGR rates in PCCI combustion mode

1023

Table 1: Technical specifications of the test engine

Engine Parameters	Specifications
Engine make/ model	AVL/ 5402
Number of cylinder/ s	1
Cylinder bore/ stroke	85 mm/ 90 mm
Swept volume	510.7 cc
Compression ratio	17.5
Inlet ports	Tangential & swirl ports
Maximum power	6.25 kW
Rated speed	4200 rpm
High pressure system	Common rail direct injection BOSCH CP4.1
Engine management system	AVL-RPEMS + BOSCH ETK7
Valves per cylinder	4 (2 inlet, 2 exhaust)
Valve train type	DOHC cam follower
Liner type/ base	Wet

1024